Cell Reports

Article

Bacillus cereus NJ01 induces SA- and ABA-mediated immunity against bacterial pathogens through the EDS1-WRKY18 module

Graphical abstract

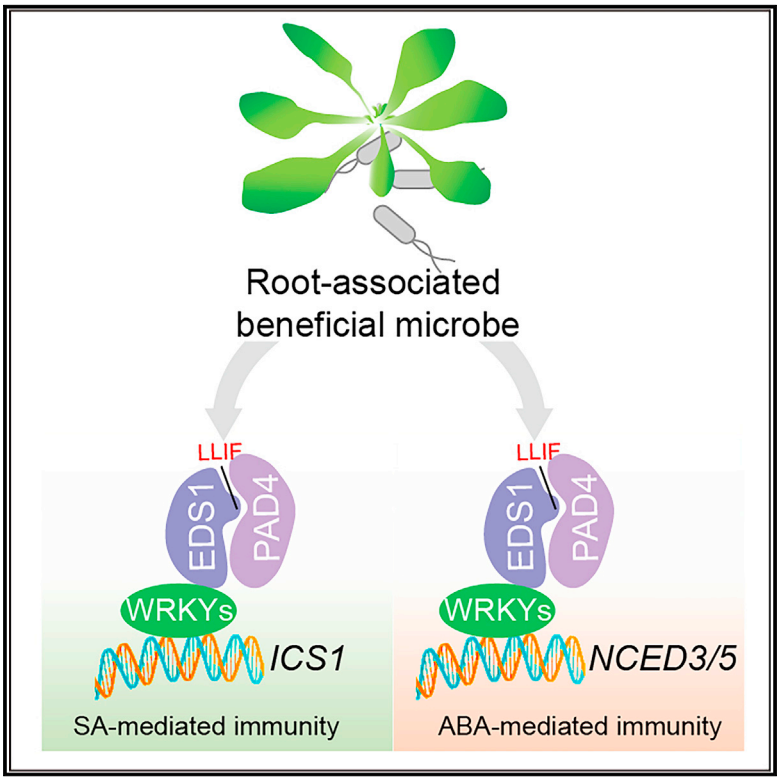

Highlights

- Rhizobacterium *Bacillus cereus* NJ01 enhances plant resistance against bacterial pathogens
- EDS1 enhances WRKY18 DNA-binding activity for the NJ01-enhanced disease resistance
- *ICS1* and *NCED3/5* are downstream of EDS1-WRKY18 for NJ01-enhanced disease resistance

Authors

Dacheng Wang, Lirong Wei, Jinbiao Ma, ..., Kenichi Tsuda, Chunhao Jiang, Yiming Wang

Correspondence

tsuda@mail.hzau.edu.cn (K.T.), chjiang@njau.edu.cn (C.J.), ymwang@njau.edu.cn (Y.W.)

In brief

The plant microbiome helps to shape the immune system to counter infection of pathogens. Wang et al. show that the root-associated *Bacillus cereus* NJ01 significantly enhances plant resistance. The EDS1-WKRY18 module is required for NJ01-enhanced disease resistance through activation of SA- and ABA-mediated immunity.

Wang et al., 2024, Cell Reports *43*, 113985
April 23, 2024
https://doi.org/10.1016/j.celrep.2024.113985

CellPress

Cell Reports

CellPress
OPEN ACCESS

Article

Bacillus cereus NJ01 induces SA- and ABA-mediated immunity against bacterial pathogens through the EDS1-WRKY18 module

Dacheng Wang,[1] Lirong Wei,[1] Jinbiao Ma,[1] Yingqiao Wan,[1] Keyi Huang,[1] Yiqiong Sun,[1] Huili Wen,[4] Zhipeng Chen,[4] Zijie Li,[1] Dongli Yu,[2] Haitao Cui,[3] Jingni Wu,[1] Yufeng Wu,[4] Sun Tae Kim,[5] Jing Zhao,[1] Jane E. Parker,[6] Kenichi Tsuda,[7,*] Chunhao Jiang,[1,*] and Yiming Wang[1,8,*]

[1]Department of Plant Pathology, Key Laboratory of Integrated Management of Crop Diseases and Pests, Ministry of Education, Nanjing Agricultural University, Nanjing 210095, China

[2]Department of Medical Oncology, Dana-Farber Cancer Institute, Harvard Medical School, Boston, MA 02115, USA

[3]Department of Plant Pathology, College of Plant Protection, Shandong Agricultural University, Tai'an, Shandong 271018, China

[4]State Key Laboratory for Crop Genetics and Germplasm Enhancement, Jiangsu Key Laboratory for Information Agriculture, Bioinformatics Center, Academy for Advanced Interdisciplinary Studies, Nanjing Agricultural University, Nanjing, China

[5]Department of Plant Bioscience, Life and Industry Convergence Research Institute, Pusan National University, Miryang 50463, Republic of Korea

[6]Department of Plant-Microbe Interactions, Max Planck Institute for Plant Breeding Research, 50829 Cologne, Germany

[7]State Key Laboratory of Agricultural Microbiology, College of Plant Science and Technology, Huazhong Agricultural University, Wuhan 430070, China

[8]Lead contact

*Correspondence: tsuda@mail.hzau.edu.cn (K.T.), chjiang@njau.edu.cn (C.J.), ymwang@njau.edu.cn (Y.W.)

https://doi.org/10.1016/j.celrep.2024.113985

SUMMARY

Emerging evidence suggests a beneficial role of rhizobacteria in ameliorating plant disease resistance in an environment-friendly way. In this study, we characterize a rhizobacterium, *Bacillus cereus* NJ01, that enhances bacterial pathogen resistance in rice and *Arabidopsis*. Transcriptome analyses show that root inoculation of NJ01 induces the expression of salicylic acid (SA)- and abscisic acid (ABA)-related genes in *Arabidopsis* leaves. Genetic evidence showed that *EDS1*, *PAD4*, and *WRKY18* are required for *B. cereus* NJ01-induced bacterial resistance. An EDS1-PAD4 complex interacts with WRKY18 and enhances its DNA binding activity. WRKY18 directly binds to the W box in the promoter region of the SA biosynthesis gene *ICS1* and ABA biosynthesis genes *NCED3* and *NCED5* and contributes to the NJ01-induced bacterial resistance. Taken together, our findings indicate a role of the EDS1/PAD4-WRKY18 complex in rhizobacteria-induced disease resistance.

INTRODUCTION

The plant microbiome is known to have multiple beneficial effects on plants, such as shaping the immune system, improving abiotic stress tolerance, and facilitating nutrient uptake.[1–3] Research in the past few decades has led to identification of various root-associated microbes that have protective effects on plants against a broad range of pathogens, a phenomenon that is widely termed induced systemic resistance (ISR).[4,5] These root-associated beneficial microbes are known to induce pathogen resistance without directly activating costly defenses and, thus, are believed to be one of the most promising long-term solutions for sustainable agriculture.[5–7] However, different beneficial microbes are known to enhance disease resistance through different molecular mechanisms, depending on the host plant and environmental conditions.[1–3] For instance, *Pseudomonas simiae*-mediated ISR requires jasmonic acid (JA) and ethylene components but is independent of salicylic acid (SA) accumulation and pathogenesis-related (PR) gene expression.[8] In contrast, *Bacillus subtilis* FB17 enhances resistance against *Pseudomonas syringae* pv. *tomato* DC3000 (*Pst*) in *Arabidopsis* by inducing closure of stomata to suppress the entry of pathogen in an SA- and abscisic acid (ABA)-dependent manner.[9] Similarly, both SA and ABA signaling are required for *Bacillus amyloliquefaciens* FZB42-mediated resistance against *Phytophthora nicotianae* in tobacco.[10] How SA- and ABA-mediated signaling contributes to microbes-induced disease resistance is still unclear.

Recent research has revealed that ENHANCED DISEASE SUSCEPTIBILITY 1 (EDS1) as a heterodimer with PHYTOALEXIN-DEFICIENT 4 (PAD4) or SENESCENCE-ASSOCIATED GENE 101 (SAG101) is required for plant resistance against host-adapted biotrophic pathogens.[11,12] Also, an EDS1-PAD4 pool is associated with plasma membrane-localized pattern recognition receptors and required for pathogen-associated molecular pattern (PAMPs)-triggered immunity (PTI).[12] Further studies show that

EDS1-PAD4-ADR1 and EDS1-SAG101-NRG1 modules are essential for Toll/interleukin-1 receptor nucleotide-binding leucine-rich-repeat (TNL)-mediated effector-triggered immunity (ETI) and also potentiate defenses downstream of coiled-coil nucleotide-binding leucine-rich-repeat (CNL) receptors in ETI.[13] These findings illustrate the key role of EDS1 in the regulation of both PTI and ETI responses. However, the downstream executing genes and pathways associated with EDS1-mediated immunity remain obscure.

ABA is well known for its stomatal closure-inducing activity during abiotic stress conditions.[14] ABA is synthesized by the sequential activities of zeaxanthin epoxidase (ZEP), 9-*cis*-epoxy carotenoid dioxygenase (NCED), short-chain alcohol dehydrogenase/reductase (SDR/ABA2), and aldehyde oxidase (AAO). Among these, NCED, in particular, limits the biosynthesis of ABA in leaves to regulate stomatal closure.[15] In response to PTI and *Pst* infection, *Arabidopsis* triggers stomatal closure to rapidly prevent the entry of pathogens through stomata in a short time.[16] Subsequent genetic evidence showed that this PAMP- and *Pst*-triggered stomatal closure is mainly induced by the SA signaling pathway.[16] NPR1, a key downstream component of SA signaling, is also known to function upstream of ABA biosynthesis and is required for PAMP-triggered stomatal closure, suggesting a possible connection between SA and ABA signaling in the regulation of stomatal immunity.[17] Nonetheless, an antagonistic effect of ABA and SA in bacterial resistance has been reported in *Arabidopsis thaliana* and *Arabidopsis lyrata*.[18] PBS3, an SA signaling component, was associated with ABA-mediated SA immune suppression.[18] These findings illustrate distinct yet coordinated roles of ABA and SA in the regulation of stomatal and innate immunity in *Arabidopsis*.[19] How SA- and ABA-mediated signaling are coordinated during beneficial microbe-induced disease resistance in plants still needs to be investigated.

WRKY transcription factors (TFs) are involved in both biotic and abiotic stress responses.[20,21] Among 74 WRKYs identified in *Arabidopsis*, WRKY18, WRKY40, and WRKY60, which belong to group IIa WRKY TFs, function redundantly for basal immunity modulation.[22] Genetic evidence has shown that WRKY18/40/60 exhibit a positive role in JA-mediated immunity but contribute negatively to SA-mediated immunity and *Pst* resistance.[22] Notably, WRKY18 and WRKY60 act as positive regulators, while WRKY40 contributes negatively to ABA and abiotic stress responses.[23] However, the role of these pivotal TFs in stomatal regulation is still unclear.

Here, we show that priming of root-associated *Bacillus cereus* NJ01 (hereafter NJ01) promotes bacterial resistance in rice (*Oryzae sativa*) and *Arabidopsis*. The immune core regulator EDS1, together with PAD4, but not SAG101, is required for the NJ01-induced disease resistance. EDS1 directly interacts with WRKY18 and enhances its W box binding activity for downstream gene activation. The SA biosynthesis gene *ICS1* and ABA biosynthesis genes NCED3/NCED5 function immediately downstream of the EDS1-WRKY18 module and are required for NJ01-induced disease resistance. Taken together, our findings uncover a role of an EDS1-PAD4-WRKY18 transcriptional module in NJ01-induced disease resistance, which benefits our understanding of interactions between host and beneficial rhizosphere microbes.

RESULTS

A root-associated *B. cereus* induces disease resistance in plants

Beneficial microbes play critical roles in the plant's adaption to biotic stress. To understand how these microbes increase plant immunity, we isolated 423 root-associated microbes from 3-month-old healthy rice (*O. sativa* L. Nipponbare) roots from the paddy field. Of these, we randomly selected 29 microbes belonging to *Bacillus*, *Chryseobacterium*, *Heyndrickxia*, *Stenortophomonas*, *Pseudomonas*, *Rossellomorea*, *Paenibacillus*, and *Priestia* for further characterization. These microbes were individually inoculated these microbes into the pots of 10-day-old rice seedlings by root irrigation. Plants were inoculated with *Xanthomonas oryzae* pv. *oryzae* (*Xoo*) 24 h post root irrigation. Of these 29 selected microbes, 25 improved rice resistance to *Xoo* (Figure S1; Table S1). Of these, we further selected NJ01 for detailed characterization by analyzing its efficacy against another pathogenic bacterium, *Xanthomonas oryzae* pv. *Oryzicola* (*Xoc*). Consistent with *Xoo* data, NJ01 also exhibited a strong plant-protecting activity against *Xoc* infection (Figures 1A and 1B) and induced expression of the defense-related genes *OsPR1*, *OsPR5*, and *OsPR10a* 48 and 72 h post inoculation (hpi) (Figure 1C).

Arabidopsis plant roots inoculated with NJ01 also exhibited improved resistance to *Pst* infection both after infiltration and spray inoculation (Figures 1D and 1E). However, a more substantial effect of NJ01 on resistance to *Pst* disease was observed upon the spray inoculation compared with infiltration (Figures 1D and 1E), suggesting that NJ01 enhances apoplastic immunity possibly by inhibition of *Pst*-mediated stomatal reopening in *Arabidopsis*. Notably, NJ01 did not show direct growth inhibition properties against *Pst* and *Xoc in vitro* (Figure S2). These results suggest that NJ01 enhances pathogen resistance by activating plant immunity.

Pst infection causes the closing of stomata at 1 hpi and their reopening at 3 hpi via secretion of coronatine, the functional mimetic compound of the plant hormone jasmonate isoleucine.[16] We therefore analyzed *Arabidopsis* stomatal dynamics at 3 hpi under mock (H_2O root inoculated + H_2O spray), NJ01 (NJ01 root inoculated + H_2O spray), *Pst* (H_2O root inoculated + *Pst* spray), and NJ01+*Pst* (NJ01 root inoculated + *Pst* spray) conditions (the same setting as in the following experiments). We found that NJ01 induces stomatal closure and inhibits *Pst*-induced stomatal reopening at 3 hpi (Figures 1F and 1G). Furthermore, the NJ01-mediated disease resistance and stomatal closure were still detected at 5 days post NJ01 root inoculation (Figure S3), suggesting that NJ01 has a relatively long-lasting protective effect on plants.

To understand the molecular mechanism underlying NJ01-mediated disease resistance, a transcriptome analysis was performed, using leaves of NJ01 root-inoculated *Arabidopsis* at 3 hpi. A total of 5,803 and 5,377 genes were found to be significantly ($|\log_2(\text{fold change})| > 1.0$, false discovery rate [FDR]-adjusted $p < 0.05$) up- and downregulated, respectively (Figure S4A; Table S2). Gene Ontology enrichment analysis suggested that those differentially expressed genes (DEGs) were related to defense response, the mitogen-activated protein

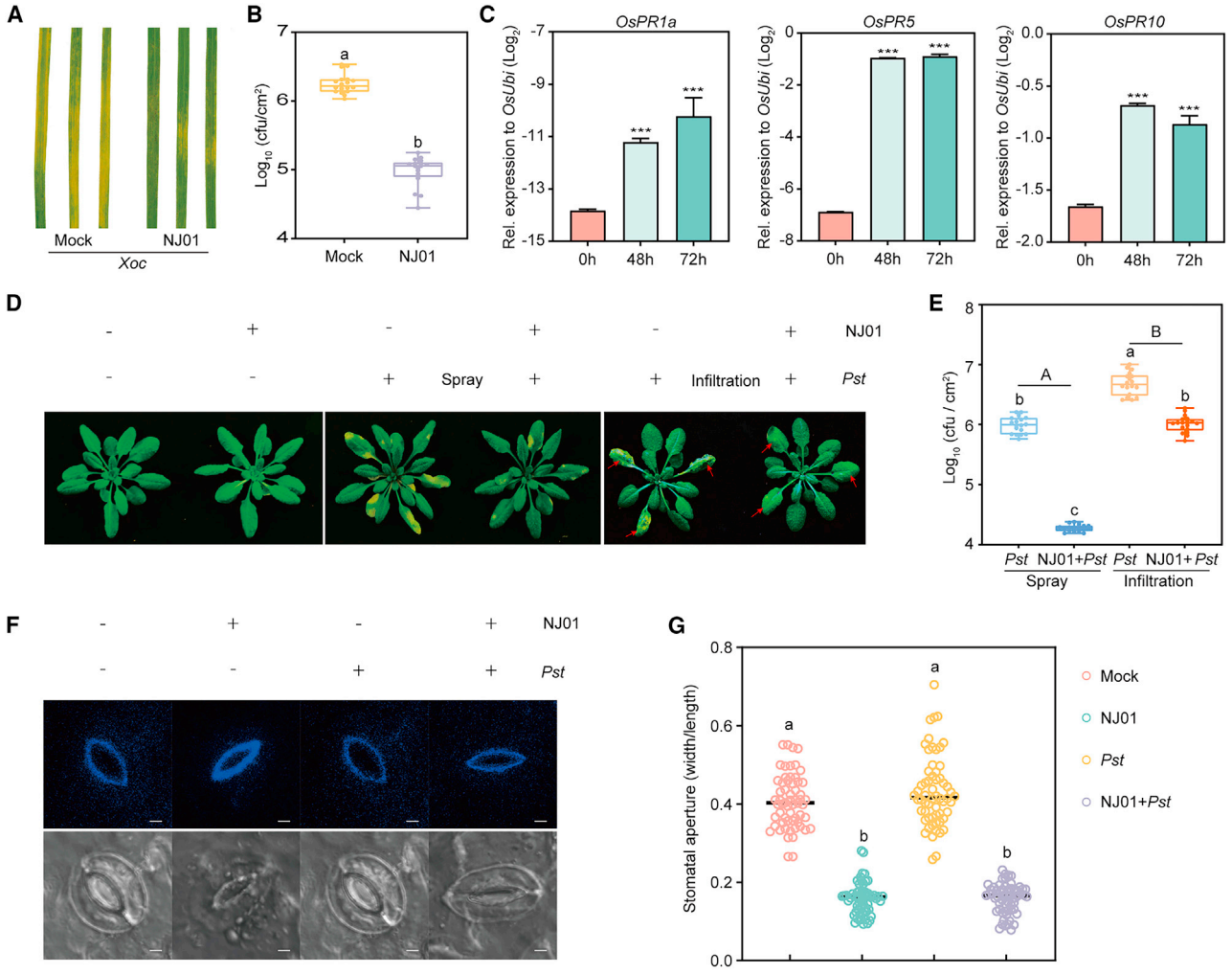

Figure 1. The root-associated *B. cereus* induces an immune response in plants

(A and B) Disease symptoms (A) and bacterial titers (B) of wild-type rice infected with *Xoc*. Ten-day-old seedlings were root inoculated with H_2O (mock) and NJ01 (optical density 600 [OD_{600}] = 0.5) and spray inoculated with *Xoc* (OD_{600} = 0.5). Disease symptoms were photographed, and bacterial titers were measured at 7 days post inoculation (dpi).

(C) Expression of *OsPR1a*, *OsPR5*, and *OsPR10* at 48 and 72 hpi with NJ01. Bars represent mean and standard error of the log_2 expression levels relative to *OsUbi*, calculated from three independent experiments, each with three biological replicates.

(D and E) Disease symptoms (D) and bacterial titers (E) of Col-0 plants infected with *Pst*. Four-week-old *Arabidopsis* plants were root inoculated with H_2O (mock) or NJ01 (OD_{600} = 0.5) and spray inoculated with *Pst* (OD_{600} = 0.2) or infiltration inoculated with *Pst* (OD_{600} = 0.001). Disease symptoms were photographed at 5 dpi, and bacterial titers were measured at 3 dpi. Red arrows indicate the *Pst*-infiltrated leaves.

(F and G) Stomatal morphology (F) and stomatal aperture (G) in leaves of Col-0 plants monitored at 3 hpi. Four-week-old *Arabidopsis* plants were root inoculated with H_2O (mock) or NJ01 (OD_{600} = 0.5) and spray-inoculated with *Pst* (OD_{600} = 0.1). The results are shown as mean ± SEM (n = 60 stomata). Different letters indicate significant differences at $p < 0.05$, as determined by one-way ANOVA with Tukey's multiple-comparisons test. Uppercase letters indicate comparisons of NJ01-induced resistance between different treatments. The experiment was performed three times with similar results. Scale bars, 5 μm.

kinase (MAPK) cascade, ISR, systemic acquired resistance, and stomatal closure (Figure S4B). These results are consistent with our finding that NJ01 enhances plant defense through the activation of stomatal and apoplastic immunity (Figures 1D and 1E). A heatmap was generated based on the transcriptional changes of DEGs, which illustrated that genes involved in plant immunity (*EDS1*, *PAD4*, and *SAG101*) and SA biosynthesis and signaling (*EDS5*, *ICS1*, *SARD1*, and *PBS3*) and WRKY TFs (*WRKY18*, *WRKY33*, *WRKY40*, and *WRKY60*) were significantly upregulated, whereas the JA signaling components *MYC3* and *MYC4* were downregulated during the activation of NJ01-mediated resistance (Figure S4C). Additionally, genes associated with ABA biosynthesis (*AAO3*, *NCED3*, and *NCED5*), perception (*PYL1*, *PYL4*, *PYL5*, *PYL6*, and *PYL7*), and signaling (*MYB2*) were also upregulated, while genes encoding for the ABA-degrading enzymes (*CYP707A1*, *CYP707A2*, and *CYP707A3*) were suppressed (Figure S3C), suggesting the involvement of SA and ABA signaling in NJ01-induced disease resistance.

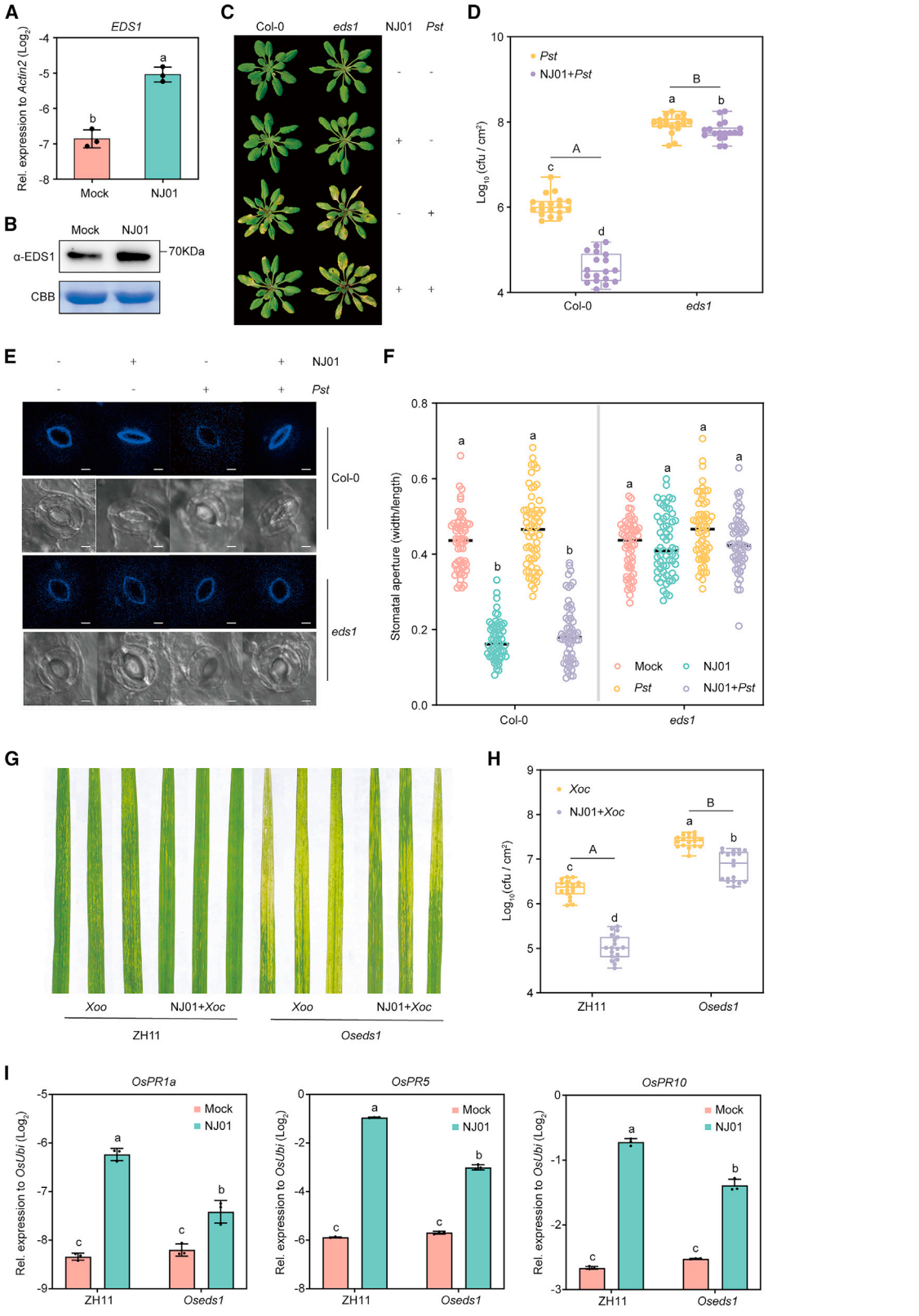

(legend on next page)

EDS1 and *PAD4* are required for NJ01-induced disease resistance

EDS1 is a key component of plant immune responses; therefore, we further validated its enhanced expression at the RNA and protein levels upon NJ01 root inoculation. As shown in Figures 2A and 2B, the transcript and protein levels of *EDS1* were significantly increased after NJ01 root inoculation, consistent with its possible role in NJ01-induced disease resistance. Notably, an *Arabidopsis eds1* loss-of-function mutant (*eds1-12*) did not exhibit NJ01-mediated *Pst* resistance or stomatal closure (Figures 2C–2F). Additionally, the rice *OsEDS1* knockout mutant (*Oseds1*), generated in the Zhonghua 11 (ZH11) background, also lacked NJ01-induced *Xoc* resistance (Figures 2G and 2H) and failed to induce *OsPR1a*, *OsPR5*, or *OsPR10* expression (Figure 2I). Taken together, these findings confirm that *EDS1* is required for NJ01-induced disease resistance in *Arabidopsis* and rice plants.

EDS1 functions in plant immunity by forming complexes with PAD4 and SAG101.[13] Transcriptome analysis showed that *PAD4* and *SAG101* were also induced upon NJ01 treatment (Figure 2). We therefore also tested whether PAD4 and SAG101 are also required for NJ01-induced disease resistance in *Arabidopsis*. Similar to the *eds1* the NJ01-induced disease resistance was also abolished in *pad4*, *pad4 sag101*, and *eds1 pad4 sag101* but not in *sag101* mutants (Figures 3A and 3B), suggesting that both EDS1 and PAD4, but not SAG101, are necessary for NJ01-induced disease resistance. The LLIF motif within an exposed EDS1 hydrophobic helix is necessary for EDS1-PAD4 heterodimer formation and EDS1-mediated ETI and PTI in *Arabidopsis*.[12,24] Therefore, we further tested whether EDS1 heterodimer formation is required for its function in NJ01-induced disease resistance by using the EDS1^{LLIF} complementation lines. Bacterial growth assays indicated that the genomic DNA of EDS1 (gEDS1-YFP) could complement *EDS1*-mediated *Pst* resistance upon NJ01 root inoculation, whereas EDS1^{LLIF}-YFP failed to exhibit this protective response (Figures 3C and 3D). Similarly, NJ01-mediated stomatal closure, which was abolished in the *eds1* mutant, was complemented by gEDS1-YFP but not by gEDS1^{LLIF}-YFP (Figures 3E and 3F). These data suggest that the EDS1-PAD4 complex contributes to the induction of NJ01-induced disease resistance in *Arabidopsis*.

WRKY18/40/60 is required for NJ01-induced disease resistance

WRKY18, *WRKY40*, and *WRKY60* were reported to function redundantly in SA-mediated immunity against bacterial pathogens in *Arabidopsis*.[22] A recent study indicated that WRKY18 is required for flg22-induced defense gene expression and ETI suppression independently of WRKY40 and WRKY60.[25] Therefore, the *wrky18* and *wrky18/40/60* triple mutants were used to dissect roles of these WRKY TFs in NJ01-induced disease resistance. Notably, NJ01-mediated *Pst* resistance and stomatal closure were significantly reduced in both the *wrky18* and *wrky18/40/60* mutants compared with Col-0 (Figures 4A–4D). Interestingly, the *wrky18* single mutant alone had a significant effect on NJ01-induced disease resistance (Figures 4A–4D), suggesting that WRKY18 can operate independently of and potentially coordinates with WRKY40 and WRKY60 in NJ01-induced disease resistance in *Arabidopsis*.

Since EDS1 and WRKY18/40/60 exhibited positive roles in NJ01-induced disease resistance, we investigated the EDS1-regulated genes are also targeted by WRKY18 and WRKY40. We re-analyzed previously published transcriptome data that reported DEGs in Col-0 and *eds1* at 0, 8, and 24 h post *Pst* AvrRps4 infection, which triggers a PTI+ETI response (Table S3),[26] and compared them with the chromatin immunoprecipitation sequencing (ChIP-seq) results of WRKY18 and WKRY40 under the flg22-induced PTI response (Table S4).[27] Although these transcriptome and ChIP-seq analyses were not performed under the same condition, this comparison may illustrate the possible relationship between EDS1- and WRKY18-regulated genes upon immune activation. Interestingly, 27 of 64 (42.2%), 2,568 of 5,829 (44.1%), and 2,951 of 7,373 (40.0%) EDS1-regulated genes were directly targeted by WRKY18 at 0, 8, and 24 hpi, respectively (Figure 4E). Moreover, 14.1%, 16.9%, and 16.4% of EDS1-regulated genes were directly regulated by WRKY40 (Figure 4F), and most of these were also targeted by WRKY18 (Figure 4F). These data suggest that WRKY18 plays a major role in EDS1-mediated transcriptional reprogramming upon pathogen infection.

EDS1 interacts with WRKY18 and affects its DNA binding activity

To investigate the relationship among EDS1, PAD4, SAG101, and WRKY18, yeast two-hybrid (Y2H) assays were performed.

Figure 2. EDS1 is required for NJ01-mediated immunity

(A) *EDS1* expression in Col-0 plants with NJ01 root inoculation. Four-week-old *Arabidopsis* plants were root inoculated with H_2O (mock) or NJ01 (OD_{600} = 0.5). Expression of *EDS1* was detected by RT-qPCR at 3 h post NJ01 root inoculation. Bars represent mean and standard error of the $\log_2$ expression levels relative to *ACTIN2*, calculated from three independent experiments, each with three biological replicates.

(B) EDS1 protein level changes after NJ01 infection in Col-0 plants, detected at 3 h post NJ01 treatment. Three independent experiments were performed with similar results.

(C and D) Disease symptoms (C) and bacterial titers (D) in Col-0 and *eds1*. Four-week-old *Arabidopsis* Col-0 and *eds1* plants were root inoculated with H_2O or NJ01 (OD_{600} = 0.5) and spray-inoculated with *Pst* (OD_{600} = 0.2). Disease symptoms (C) were photographed at 5 dpi, and bacterial titers (D) were measured at 3 dpi.

(E and F) Stomatal morphology (E) and stomatal aperture (F) in leaves of Col-0 and *eds1* root inoculated with NJ01 (OD_{600} = 0.5) and/or spray-inoculated with *Pst* (OD_{600} = 0.1). Stomatal images were taken at 3 h post inoculation (hpi). The results are shown as mean ± SEM (n = 60 stomata). Scale bars, 5 μm.

(G and H) Disease symptoms (G) and bacterial titers (H) of wild-type rice infected with *Xoc*. Ten-day-old seedlings were root inoculated with H_2O and NJ01 (OD_{600} = 0.5) and spray inoculated with *Xoc* (OD_{600} = 0.5). Disease symptoms were photographed, and bacterial titers were measured at 7 dpi.

(I) Expression of *OsPR1*, *OsPR5*, and *OsPR10a* in wild-type (ZH11) and *Oseds1* plants was detected by RT-qPCR at 48 hpi. Ten-day-old seedlings were root inoculated with H_2O (mock) and NJ01 (OD_{600} = 0.5). Bars represent mean and standard error of the $\log_2$ expression levels relative to *OsUbi*, calculated from three independent experiments, each with three biological replicates. Different letters indicate significant differences at $p < 0.05$, as determined by one-way ANOVA with Tukey's multiple-comparisons test. Uppercase letters indicate comparisons between genotypes for disease resistance. The experiment was performed three times with similar results.

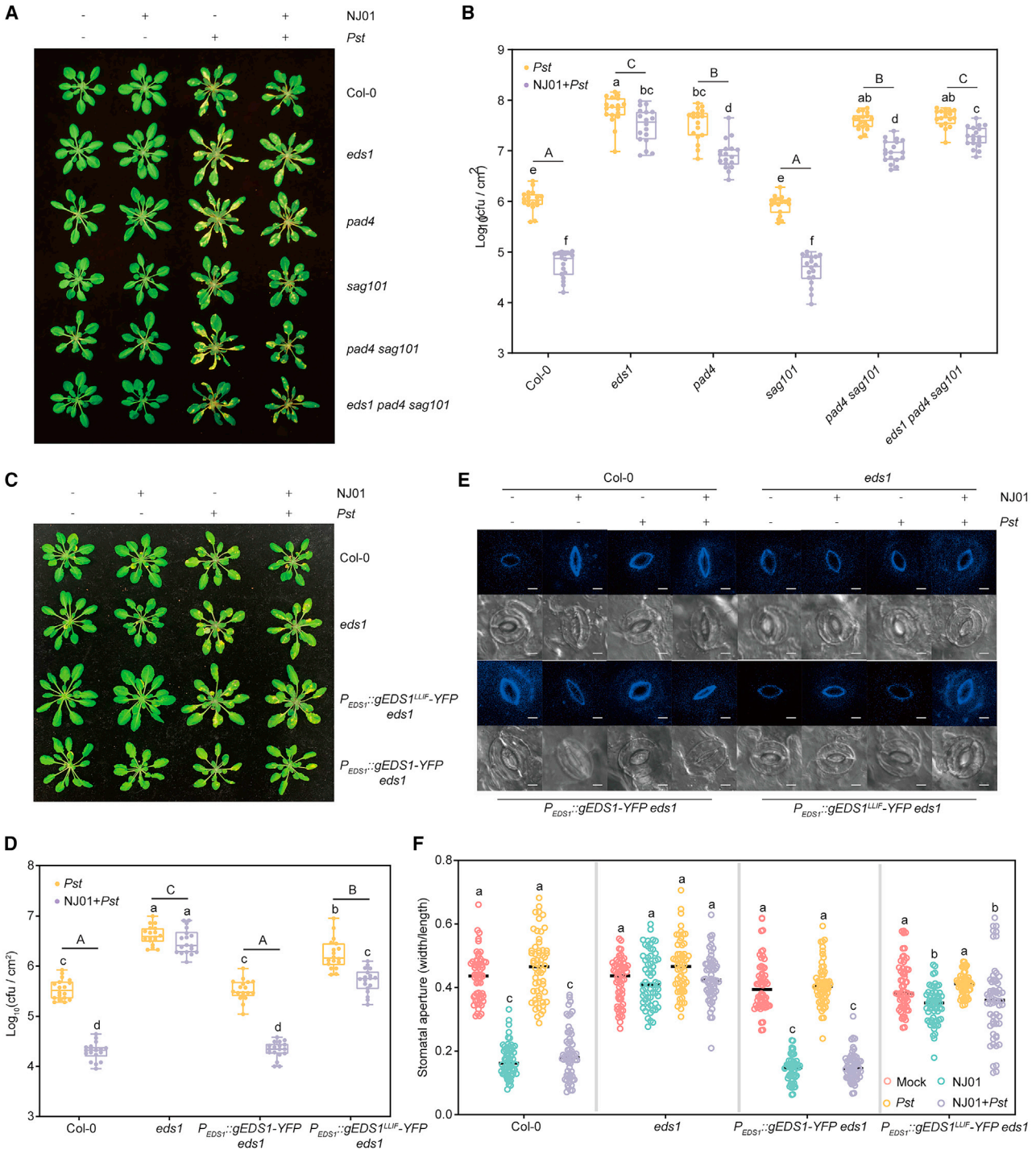

Figure 3. PAD4, but not SAG101, is required for NJU01-mediated immunity

(A and B) Disease symptoms (A) and bacterial titers (B) in Col-0, *eds1*, *pad4, sag101*, *pad4 sag101*, and *eds1 pad4 sag101*.

(C and D) Disease symptoms (C) and bacterial titers (D) in Col-0, *eds1*, P_{EDS1}*::gEDS1-YFP eds1*, and P_{EDS1}*::gEDS1*^{LLIF}*-YFP eds1*. Four-week-old *Arabidopsis* plants were root inoculated with H_2O or NJ01 (OD_{600} = 0.5) and spray inoculated with *Pst* (OD_{600} = 0.2).

(A–D) Disease symptoms (A and C) were photographed at 5 dpi, and bacterial titers (B and D) were measured at 3 dpi.

(E and F) Stomatal morphology (E) and stomatal aperture (F) in leaves of Col-0, *eds1*, P_{EDS1}*::gEDS1-YFP eds1*, and P_{EDS1}*::gEDS1*^{LLIF}*-YFP eds1*. Four-week-old plants were root inoculated with NJ01 (OD_{600} = 0.5) and/or spray-inoculated with *Pst* (OD_{600} = 0.1). Stomatal images were taken at 3 hpi. The results are shown as mean ± SEM (n = 60 stomata). Different letters indicate significant differences at $p < 0.05$, as determined by one-way ANOVA with Tukey's multiple-comparisons test. Uppercase letters indicate comparisons between genotypes for disease resistance. The experiment was performed three times with similar results. Scale bars, 5 μm.

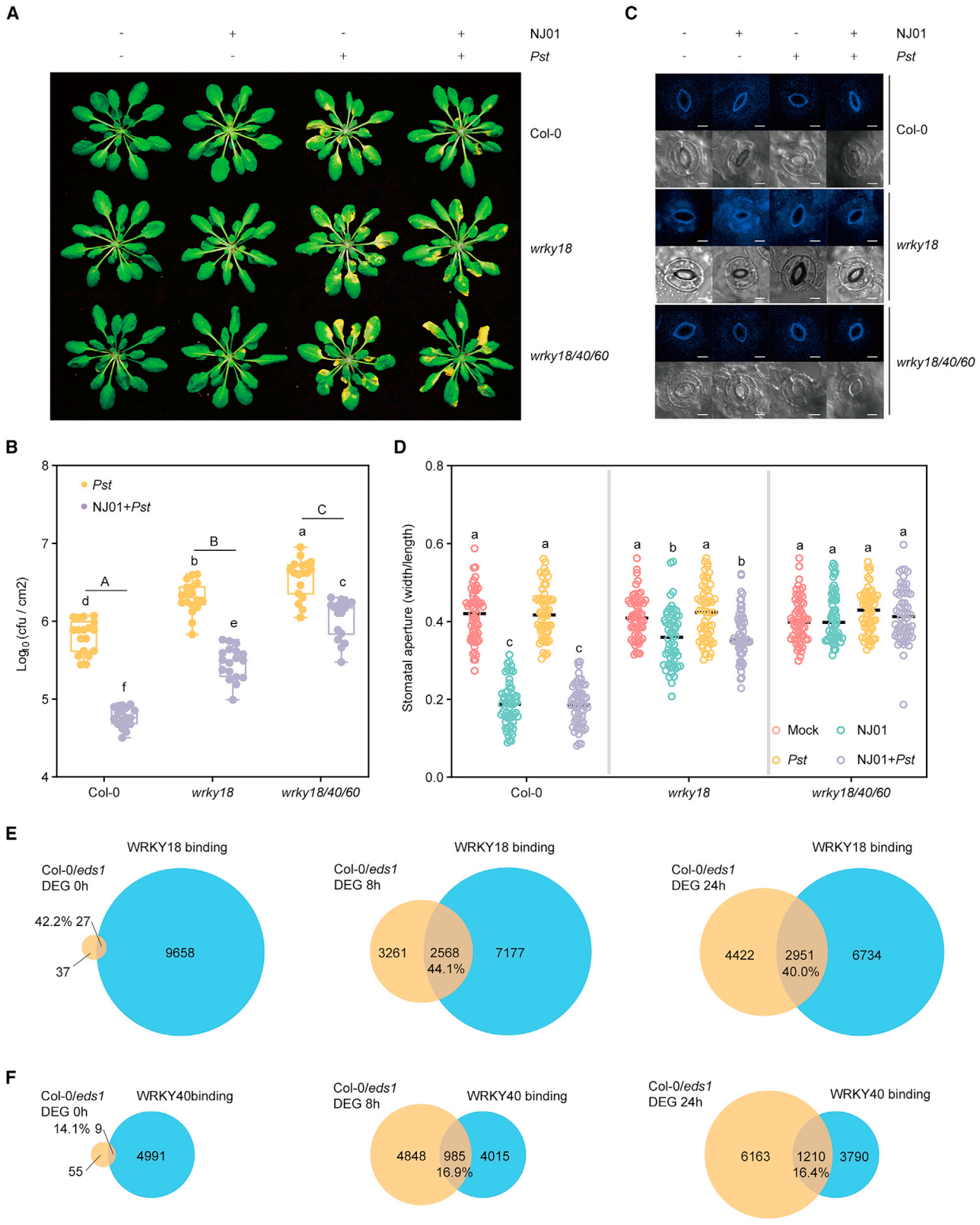

(legend on next page)

The Y2H results indicated a direct interaction of EDS1 with WRKY18, while PAD4 and SAG101 did not show such interaction (Figure 5A). Subsequent bimolecular fluorescence complementation (BiFC) analysis, however, indicated that both EDS1 and PAD4 interact with WRKY18 in the nucleus (Figure 5B). A co-immunoprecipitation (coIP) analysis was further performed by using P_{WRKY18}::*WRKY18-HA wrky18* plants. As shown in Figure 5C, EDS1 and PAD4, but not SAG101, could be co-precipitated by WRKY18 in plants, suggesting that EDS1-PAD4 may form a complex with WRKY18 through the direct interaction between EDS1-PAD4 and EDS1-WRKY18. These results are consistent with the genetic evidence showing that *EDS1*, *PAD4*, and *WRKY18*, but not *SAG101*, are required for NJ01-induced disease resistance.

The EDS1-PAD4 heterodimer inhibited the DNA binding activity of MYC2 in plants,[28] suggesting that the EDS1-PAD4 complex may regulate the biochemical functions of certain TFs. We therefore analyzed whether the interaction of EDS1 with WRKY18 affects WRKY18 DNA binding activity. Microscale thermophoresis (MST) analysis showed that WRKY18 directly binds to the W box sequence of *NCED5* (K_d = 86.26 μM) (Figure 5D) but not the mutated W box (Figure S5A). In the presence of EDS1, the DNA binding activity of WRKY18 was increased to K_d = 17.93 μM (Figure 5D). These findings were further validated by an electrophoretic mobility shift assay (EMSA). Recombinant WRKY18 bound to the NCED5 promoter containing a W box (Figures 5E; Figure S5B). This binding was significantly enhanced by EDS1-glutathione S-transferase (GST) recombinant protein compared with GST alone (Figure 5E). These results suggest that EDS1 enhances the DNA binding affinity of WRKY18.

EDS1-WRKY18 directly regulates NJ01-mediated SA and ABA biosynthesis

SA signaling plays a major role in plant immunity. A previous ChIP-seq analysis showed that WRKY18 directly targets the W box in the isochorismate synthase 1 (*ICS1*) promoter region upon flg22 treatment of *Arabidopsis*,[27] suggesting that WRKY18 may regulate SA biosynthesis through *ICS1*. We observed that NJ01 induces the expression of *ICS1*, which is partially reduced in *eds1* and *wrky18/40/60* mutants (Figure 6A). *gEDS1-YFP* but not *gEDS1*^{LLIF}*-YPF* partially rescued the NJ01-triggered *ICS1* expression (Figure 6A). Moreover, a direct binding of WRKY18 to the promoter region of *ICS1* was observed (Figure 6B). Accordingly, the NJ01-triggered SA accumulation was reduced in *eds1* and *wrky18/40/60* (Figure 6C), while the NJ01-induced *Pst* resistance and stomatal closure were partially abolished in an *ics1* (*sid2*) mutant (Figures 6D–6G).

Promoter analysis indicated that a W box is present at −2,621-bp and −1,706-bp positions in the promoter regions of *NCED3* and *NCED5*, respectively which suggested that *NCED3/5* may be direct targets of *WRKY18/40/60* and function downstream of *EDS1*. Indeed, NJ01-induced expression of *NCED3* and *NCED5* was significantly reduced in *eds1* and *wrky18/40/60* compared with that of Col-0 (Figures 7A and 7B). The reduced expression of *NCED3* and *NCED5* in *eds1* was fully complemented by *gEDS1-YFP* and partially by *gEDS1*^{LLIF}*-YFP*, suggesting that the LLIF domain, and thus EDS1 association with PAD4, contributes to EDS1-mediated *NCED3/5* expression (Figures 7A and 7B). Our results further showed that WRKY18 directly binds to the promoter region of *NCED3* and *NCED5* (Figures 7C and 7D). Additionally, the *eds1* and *wrky18/40/60* mutants displayed reduced ABA content after mock treatment, and NJ01 treatment failed to compensate the reduced basal ABA level in these mutants (Figure 7E). Upon NJ01 inoculation, ABA accumulation was even lower in *eds1* and *wrky18/40/60* compared with Col-0 (Figure 7E). The NJ01-induced *Pst* resistance and stomatal closure were also partially compromised in an *nced3/5* double mutant (Figures 7F–7I). Taken together, our data show that an EDS1-WRKY18 module contributes to both SA- and ABA-mediated immunity during NJ01-induced disease resistance.

DISCUSSION

Root-associated microbes exhibit protective effects on plants against a broad range of pathogens.[1–3] However, knowledge of the regulatory networks associated with beneficial microbe-induced disease resistance is fragmentary. In the present study, we demonstrate that EDS1 is an important component of the *Bacillus*-induced disease resistance in both rice and *Arabidopsis*. Further genetic and biochemical evidence in *Arabidopsis* illustrates that WRKY18 functions downstream of EDS1-PAD4 dimers and contributes to the induction of SA- and ABA-mediated immunity in NJ01-induced disease resistance (Figure S6).

Previous reports have shown that EDS1 physically interacts with PAD4 or SAG101 and is required for PTI, ETI, and systemic acquired resistance (SAR) in plants.[29–31] EDS1 participates in SA-dependent as well as SA-independent pathways in defense gene expression and pathogen resistance.[29,31,32] However, the molecular mechanism underlying EDS1-mediated downstream transcriptional reprogramming remained unclear. WRKY TFs are required for large-scale transcriptional reprogramming in

Figure 4. WRKY18/40/60 is required for NJ01-mediated plant immunity

(A and B) Disease symptoms (A) and bacterial titers (B) of Col-0, *wrky18*, and *wrky18/40/60* plants root inoculated with H_2O or NJ01 (OD_{600} = 0.5) and spray inoculated with *Pst* (OD_{600} = 0.2). Disease symptoms were photographed at 5 dpi, and bacterial titers were measured at 3 dpi.

(C and D) Stomatal morphology (C) and stomatal aperture (D) in leaves of Col-0, *wrky18*, and *wrky18/40/60 plants* root inoculated with NJ01 (OD_{600} = 0.5) and/or spray-inoculated with *Pst* (OD_{600} = 0.1). Stomatal images were taken at 3 hpi. The results are shown as mean ± SEM (n = 60 stomata). Different letters indicate significant differences at $p < 0.05$, as determined by one-way ANOVA with Tukey's multiple-comparisons test. Uppercase letters indicate comparisons between genotypes for disease resistance. The experiment was performed three times with similar results. Scale bars, 5 μm.

(E and F) Bioinformatics analysis of gene regulation of EDS1 with WRKY18 (E) and WRKY40 (F). DEGs in Col-0 and *eds1* at 0, 8, and 24 h post *Pst* AvrRps4 infection from a previous publication (Bhandari et al.,[26] yellow) were compared with the ChIP-seq results of WRKY18 and WRKY40 upon flg22 treatment (Birkenbihl et al.,[27] blue). Co-regulated gene numbers are indicated. The percentage indicates the ratio of DEGs in *eds1* directly regulated by WRKY TFs.

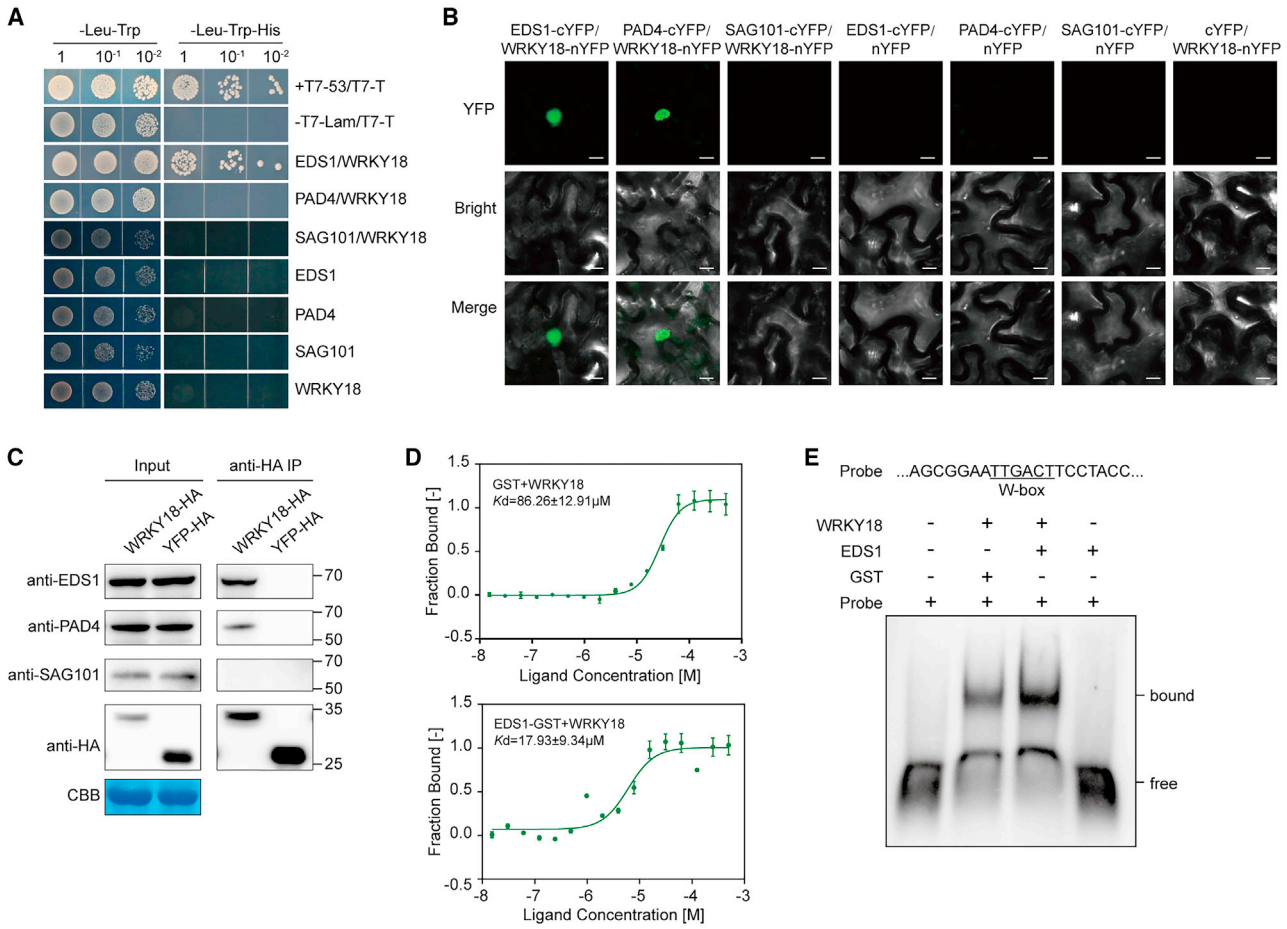

Figure 5. EDS1 interacts with WRKY18 and affects its DNA-binding activity

(A) Y2H assay of interaction between EDS1, PAD4, SAG101, and WRKY18. BD-WRKY18 plasmids were co-transformed with AD-EDS1, AD-PAD4, or AD-SAG101 into yeast cells and screened on synthetic dextrose medium lacking leucine and tryptophan (−Leu−Trp) or lacking leucine, tryptophan, and histidine (−Leu−Trp−His). pGADT7-T + pGBKT7-53 was used as a positive control. pGADT7 + pGBKT7-lam was used as a negative control.

(B) BiFC assay of EDS1, PAD4, SAG101, and WRKY18. EDS1, PAD4, or SAG101 was fused to the C-terminal portion of YFP, and WRKY18 was fused to the N-terminal portion of YFP, and they were co-expressed in *N. benthamiana* leaves. Images were obtained using a confocal laser-scanning microscope at 3 dpi. Scale bars, 10 μm.

(C) CoIP of WRKY18 with EDS1, PAD4, and SAG101 in *Arabidopsis*. Plants expressing P_{WRKY18}:*WRKY18-HA* were immunoprecipitated with an anti-hemagglutinin (HA) monoclonal antibody. Accumulation of EDS1, PAD4, and SAG101 was detected using anti-EDS1, anti-PAD4, and anti-SAG101 antibodies, respectively. Plants expressing P_{35S}:*YFP-HA* were used as a negative control. Equal sample loading on the blot was estimated with Ponceau S staining.

(D and E) EDS1 enhances WRKY18 transcriptional activity to bind to the W box (5′-CATTCGTAGCGGAATTGACTTCCTACCGATCTT-3′) in microscale thermophoresis (MST) assays (D) and (5′-AGCGGAATTGACTTCCTACCGATCTT-3′) in the EMSA (E). The dissociation curve was fit to the data to calculate the K_d values.

plants during pathogen infection.[33] Here, we provide evidence for a link between immune core regulator EDS1 and defense-related TF WRKY18 during the mobilization of NJ01-induced disease resistance. Our data show that EDS1 and PAD4 form a complex with WRKY18 and affect its function in immune activation (Figure 4). The EDS1-PAD4-ADR1 node has been shown to be required for receptor-like protein 23 (RLP23)-mediated ethylene production, reactive oxygen species (ROS) burst, callose deposition, and *Pst* resistance.[12] Furthermore, protein pool of the EDS1-PAD4-ADR1 node has been shown to be spatially close to the plasma membrane-localized RLP23-SOBIR1 complex.[12] Here, we show that both *EDS1* and *PAD4* are required for the NJ01-induced disease resistance, while *SAG101*, which is required for EDS1-mediated ETI activation, is not associated with the NJ01-induced disease resistance. Although WRKY18 did not show direct interaction in Y2H analysis with PAD4, it is possible that the EDS1-PAD4 complex, but not PAD4 alone, interacts with and influences WRKY18 functions in the nucleus for defense transcription reprogramming in *Arabidopsis*.

A previous report has shown an antagonistic effect of ABA and SA on bacterial resistance in *Arabidopsis*.[18] However, those results were observed after inoculation of *Pst* by infiltration, which bypasses engagement of stomatal immunity. Our

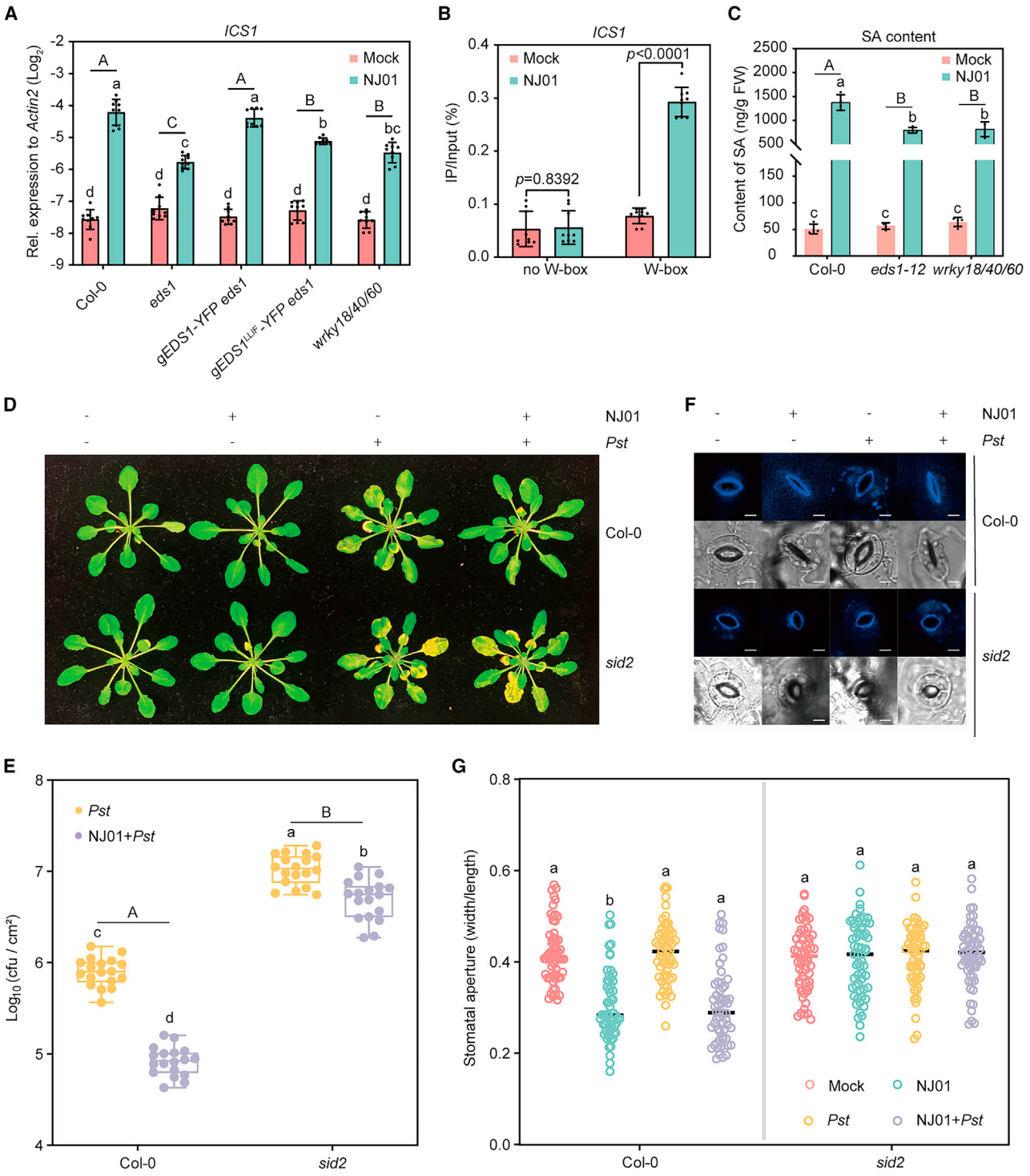

Figure 6. *ICS1* is directly regulated by EDS1-WRKY18 and required for full NJ01-mediated plant immunity

(A) Expression of *ICS1* in leaves of Col-0, *eds1*, *gEDS1-YFP eds1*, *gEDS1*^{LLIF}*-YFP eds1*, and *wrky18/40/60* plants at 3 hpi post root-irrigation of H_2O (mock) or NJ01 (OD_{600} = 0.5). Bars represent mean and standard error of the $\log_2$ expression levels relative to *ACTIN2*, calculated from three independent experiments each, with three biological replicates.

(B) ChIP-qPCR analysis of binding of WRKY18-HA to the W box motif of the SA biosynthesis gene *ICS1*. Two-week-old P_{WRKY18}*::WRKY18-HA wrky18* seedlings were pretreated with H_2O (mock) or NJ01 for 3 h.

(legend continued on next page)

results showed that both SA and ABA are required for the NJ01-mediated immunity. This is consistent with a previous report showing that the SA signaling component NPR1 functions upstream of ABA signaling and is required for the PAMP-triggered stomatal closure.[17] More recently, it has been shown that the EDS1-PAD4 complex is required for flg22-triggered stomatal immunity by inducing SA and ABA biosynthesis via operating of NbWRKY40e.[34] Therefore, it is likely that SA and ABA exhibit antagonistic effects on the apoplast or mesophyll cells in pathogen resistance and synergistic effects on regulating stomatal closure.

WRKY18, WRKY40, and WRKY60 are functionally redundant and contribute negatively to basal immunity in *Arabidopsis*.[22] However, WRKY18 was also required for *Pst* resistance under BTH- and PAMP-mediated priming conditions[25,35] and positively contributed to SAR in *Arabidopsis*.[35] Moreover, WRKY18 and WRKY60 are known to positively regulate the ABA and abiotic stress responses in plants, while WRKY40 negatively regulates these responses negatively.[23,36,37] Here, we report that WRKY18, WRKY40, and WRKY60 have coordinated activities for SA and ABA biosynthesis in *Arabidopsis* upon NJ01 treatment, in line with NbWRKY40e being required for pathogen-induced SA and ABA biosynthesis in *Nicotiana benthamiana*.[34] These results indicate that the regulatory roles of WRKY18, WRKY40, and WRKY60 are more intricate and varied in plants in response to different stresses.

Systemic resistance emerges as an important mechanism for enhanced defense against a broad range of pathogens and insect herbivores.[5] However, compared with ETI and basal immunity, the molecular mechanism underlying systemic resistance is still elusive and needs to be further dissected. Previous studies have shown that the absence of NPR1, the main positive regulator of SA-mediated immunity, leads to the loss of ISR in *Arabidopsis*,[8] which points to the importance of SA in ISR in plants. TFs such as WRKY8, WRKY33, WRKY11, WRKY70, MYC2, and MYB72 have been reported to be required for systemic resistance in *Arabidopsis*.[21,38–40] Notably, most of these are associated with the JA-mediated signaling pathway and iron homeostasis, and only WRKY70 has been linked to SA-mediated signaling pathways. Both SA and ABA were required for *Bacillus*-induced stomatal closure and pathogen resistance in *Arabidopsis*.[9,10] However, the underlying regulatory signaling network is still unclear. Consistent with the previous findings, we discovered that both SA and ABA are also required for NJ01-induced disease resistance. Genetic and phytohormone profiling evidence demonstrated that the EDS1-WRKY18 module promotes increases in SA and ABA accumulation through direct activation of their biosynthetic genes *ICS1* and *NCED3/5*, respectively (Figures 6, 7, and S6). The fact that the NJ01-induced disease resistance is totally abolished in *eds1* but partially compromised in the *sid2* and *nced3/5* mutants suggests that both SA and ABA are downstream executors of EDS1 for coordinating NJ01-induced disease resistance downstrwam of EDS1. Interestingly, it was reported that both NPR1 and WRKY18 are required for the activation of SA-mediated SAR in *Arabidopsis*.[35] Therefore, it is more likely that NJ01 employs the SAR pathway to enhance pathogen resistance. Taken together, our findings provide the missing link of how SA and ABA are regulated and coordinated in shaping the systemic resistance in plants.

Limitations of the study

In this study, we have uncovered a protective role of root-associated beneficial microbe *B. cereus* NJ01 in plants against pathogen infection. However, it is essential to highlight certain limitations in our analysis. First, a field test is lacking to understand whether NJ01 activity is relevant in nature where it would likely exist in a microbial community. Second, as *sid2* and *nced3 nced5* mutants partially reduce the NJ01-induced disease resistance, experiments utilizing a triple mutant of *sid2 nced3 nced5* might clarify whether SA and ABA are coordinated for NJ01-induced disease resistance in *Arabidopsis*.

STAR★METHODS

Detailed methods are provided in the online version of this paper and include the following:

- KEY RESOURCES TABLE
- RESOURCE AVAILABILITY
  - Lead contact
  - Materials availability
  - Data and code availability
- EXPERIMENTAL MODEL AND SUBJECT PARTICIPANT DETAILS
  - Plant materials and growth conditions
- METHOD DETAILS
  - Bacterial strains, infection and bacterial growth analysis
  - RNA extraction and qPCR analysis
  - Stomatal apartural analysis
  - Transcriptome and data analysis
  - RNA-seq and ChIP-seq re-analysis processing
  - Protein extraction and immunoblot analysis
  - Bimolecular fluorescence complementation (BiFC) assay
  - Co-immunoprecipitation (Co-IP)

(C) SA contents in Col-0, *eds1*, and *wrky18/40/60* root inoculated with H_2O and NJ01 (OD_{600} = 0.5) at 3 hpi. Different letters indicate significant differences at $p < 0.05$, as determined by one-way ANOVA with Tukey's multiple-comparisons test. Bars represent the mean and standard error of four independent biological replicates.

(D and E) Disease symptoms (D) and bacterial titers (E) in Col-0 and *sid2*. Four-week-old *Arabidopsis* Col-0 and *sid2* plants were root inoculated with H_2O or NJ01 (OD_{600} = 0.5) and spray inoculated with *Pst* (OD_{600} = 0.2). Disease symptoms (D) were photographed at 5 dpi, and bacterial titers (E) were measured at 3 dpi.

(F and G) Stomatal aperture in leaves of Col-0 and *sid2* root inoculated with NJ01 (OD_{600} = 0.5) and/or spray inoculated with *Pst* (OD_{600} = 0.1). Stomatal images were taken at 3 hpi. The results are shown as mean ± SEM (n = 60 stomata). Different letters indicate significant differences at $p < 0.05$, as determined by one-way ANOVA with Tukey's multiple-comparisons test. Uppercase letters indicate comparisons between genotypes. The experiment was performed three times with similar results. Scale bars, 5 μm.

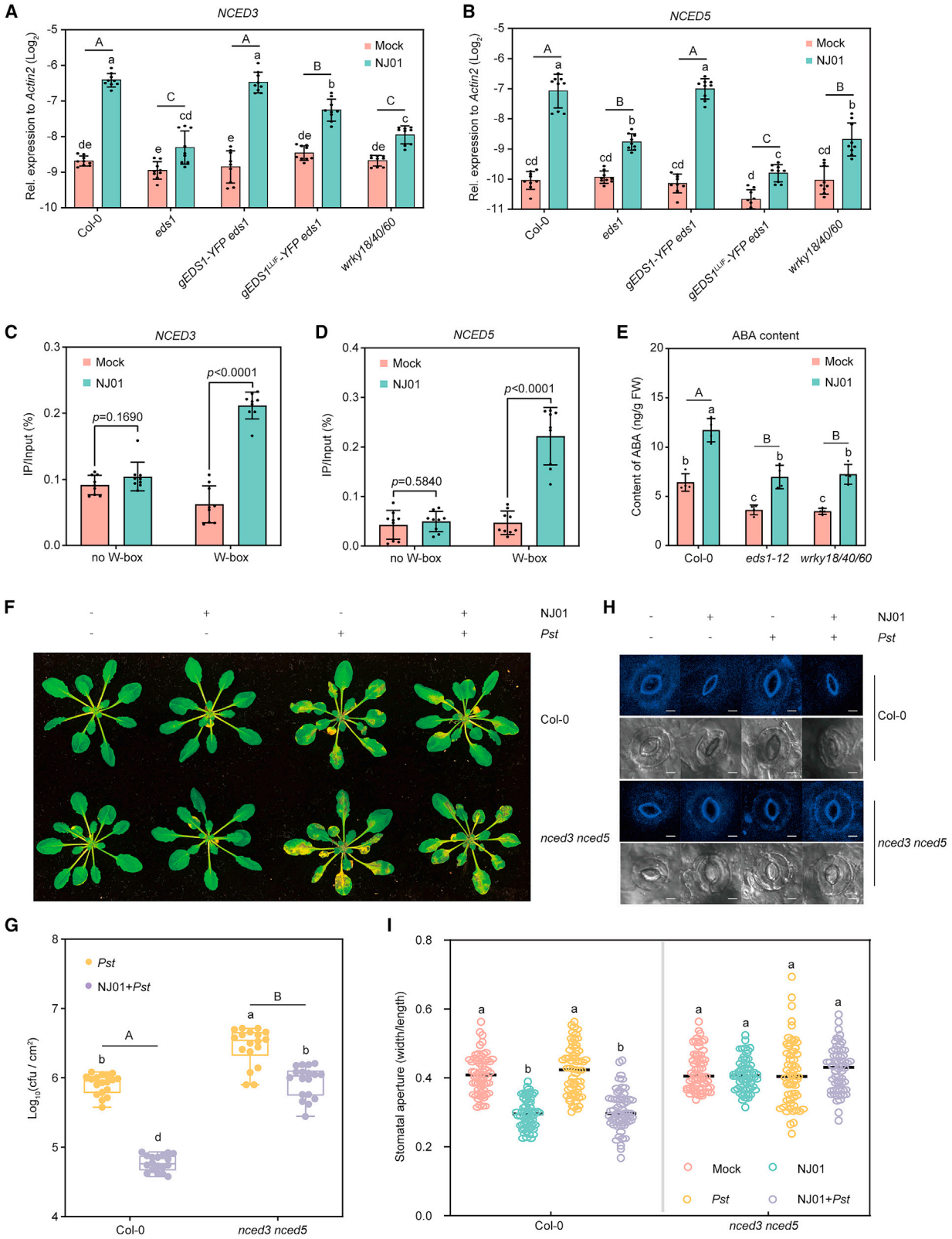

(legend on next page)

- Chromatin immunoprecipitation (ChIP) assay
- Yeast-two-hybride assay
- Microscale thermophoresis (MST) analysis
- Electrophoresis mobility shift assay (EMSA)
- Determination of phytohormone levels
- Accession numbers

● QUANTIFICATION AND STATISTICAL ANALYSIS

SUPPLEMENTAL INFORMATION

Supplemental information can be found online at https://doi.org/10.1016/j.celrep.2024.113985.

ACKNOWLEDGMENTS

We thank Prof. Imore Somssich for providing the *wrky18/40/60*, *35S::WRKY18-HA*, and *nced3 nced5* mutants. This work was supported by the National Natural Science Foundation of China (grants 32202382, 31970281, and 32172420), the National Key Research and Development Project (grants 2022YFE0198100 and 2022YFD1400100), the Natural Science Foundation of Jiangsu Province (grant SBK20220085), the Fundamental Research Funds for the Central Universities (KJJQ2023001), the Agricultural Technology Innovation Fund of Jurong (ZA32205), the National Research Foundation of Korea funded by the Ministry of Education, Science, and Technology (grant 2021K1A3A1A61003041 to S.T.K.), and Sino-German Mobility Grant (M-0275 to J.E.P. and H.C.)

AUTHOR CONTRIBUTIONS

Y. Wang, C.J., and K.T. designed the research. D.W., L.W., J.M., Y. Wan, K.H., Y.S., Z.C., Z.L., D.Y., H.C., and J.W. carried out the experiments. Y. Wu, D.W., H.W., J.Z., S.T.K., K.T., J.P., C.J., and Y. Wang analyzed the data and wrote the manuscript. All authors commented on and finalized the manuscript.

DECLARATION OF INTERESTS

The authors declare no competing interests.

Received: October 22, 2023
Revised: January 22, 2024
Accepted: March 6, 2024
Published: March 21, 2024

REFERENCES

1. Hiruma, K., Gerlach, N., Sacristán, S., Nakano, R.T., Hacquard, S., Kracher, B., Neumann, U., Ramírez, D., Bucher, M., O'Connell, R.J., and Schulze-Lefert, P. (2016). Root endophyte colletotrichum tofieldiae confers plant fitness benefits that are phosphate status dependent. Cell *165*, 464–474.
2. Morcillo, R.J., Singh, S.K., He, D., An, G., Vílchez, J.I., Tang, K., Yuan, F., Sun, Y., Shao, C., Zhang, S., et al. (2020). Rhizobacterium-derived diacetyl modulates plant immunity in a phosphate-dependent manner. EMBO J. *39*, e102602.
3. Andrés-Barrao, C., Alzubaidy, H., Jalal, R., Mariappan, K.G., de Zélicourt, A., Bokhari, A., Artyukh, O., Alwutayd, K., Rawat, A., Shekhawat, K., et al. (2021). Coordinated bacterial and plant sulfur metabolism in *Enterobacter* sp. SA187–induced plant salt stress tolerance. USAProc. Natl. Acad. Sci. USA *118*, e2107417118.
4. Heil, M., and Bostock, R.M. (2002). Induced systemic resistance (ISR) against pathogens in the context of induced plant defenses. Ann. Bot. *89*, 503–512.
5. Pieterse, C.M.J., Zamioudis, C., Berendsen, R.L., Weller, D.M., Van Wees, S.C.M., and Bakker, P.A.H.M. (2014). Induced systemic resistance by beneficial microbes. Annu. Rev. Phytopathol. *52*, 347–375.
6. Chen, Q.L., Hu, H.W., He, Z.Y., Cui, L., Zhu, Y.G., and He, J.Z. (2021). Potential of indigenous crop microbiomes for sustainable agriculture. Nat. Food *2*, 233–240.
7. Singh, B.K., Trivedi, P., Egidi, E., Macdonald, C.A., and Delgado-Baquerizo, M. (2020). Crop microbiome and sustainable agriculture. Nat. Rev. Microbiol. *18*, 601–602.
8. Pieterse, C.M., van Wees, S.C., van Pelt, J.A., Knoester, M., Laan, R., Gerrits, H., Weisbeek, P.J., and van Loon, L.C. (1998). A novel signaling pathway controlling induced systemic resistance in Arabidopsis. Plant Cell *10*, 1571–1580.
9. Kumar, A.S., Lakshmanan, V., Caplan, J.L., Powell, D., Czymmek, K.J., Levia, D.F., and Bais, H.P. (2012). Rhizobacteria *Bacillus subtilis* restricts foliar pathogen entry through stomata. Plant J. *72*, 694–706.
10. Wu, L., Huang, Z., Li, X., Ma, L., Gu, Q., Wu, H., Liu, J., Borriss, R., Wu, Z., and Gao, X. (2018). Stomatal closure and SA-JA/ET-signaling pathways are essential for *Bacillus amyloliquefaciens* FZB42 to restrict leaf disease caused by *Phytophthora nicotianae* in Nicotiana benthamiana. Front. Microbiol. *9*, 847.
11. Ganter, J., Ordon, J., Kretschmer, C., Guerois, R., and Stuttmann, J. (2019). An EDS1-SAG101 complex is essential for TNL-mediated immunity in Nicotiana benthamiana. Plant Cell *31*, 2456–2474.
12. Pruitt, R.N., Locci, F., Wanke, F., Zhang, L., Saile, S.C., Joe, A., Karelina, D., Hua, C., Fröhlich, K., Wan, E.L., et al. (2021). The EDS1-PAD4-ADR1 node mediates Arabidopsis partern-triggered immunity. Nature *598*, 459–499.
13. Chang, M., Chen, H., Liu, F., and Fu, Z.Q. (2022). PTI and ETI: convergent pathways with diverse elicitors. Trends Plant Sci. *27*, 113–115.
14. Cai, S., Chen, G., Wang, Y., Huang, Y., Marchant, D.B., Wang, Y., Yang, Q., Dai, F., Hills, A., Franks, P.J., et al. (2017). Evolutionary Conservation of ABA signaling for stomatal closure. Plant Physiol. *174*, 732–747.
15. Xiong, L., and Zhu, J.K. (2003). Regulation of abscisic acid biosynthesis. Plant Physiol. *133*, 29–36.

Figure 7. *NCED3/NCED5* are directly regulated by EDS1-WRKY18 and are required for full NJ01-mediated immunity

(A and B) Expression of *NCED3* and *NCED5* in leaves of Col-0, *eds1*, *gEDS1-YFP eds1*, *gEDS1^{LLIF}-YFP eds1*, and *wrky18/40/60* plants at 3 hpi post root-irrigation of H_2O (mock) or NJ01 (OD_{600} = 0.5). Bars represent mean and standard error of the $\log_2$ expression levels relative to *ACTIN2*, calculated from three independent experiments, each with three biological replicates.

(C and D) ChIP-qPCR analysis of binding of WRKY18-HA to the W-box motif from the ABA biosynthetic genes *NCED3* and *NCED5*. Two-week-old P_{WRKY18}*::WRKY18-HA wrky18* seedlings were pretreated with H_2O (mock) or NJ01 for 3 h.

(E) ABA contents in Col-0, *eds1*, and *wrky18/40/60* root inoculated with H_2O and NJ01 (OD_{600} = 0.5) at 3 hpi. Bars represent the mean and standard error of four independent biological replicates.

(F and G) Disease symptoms (F) were photographed and bacterial titers (G) of Col-0 and *nced3 nced5* plants root inoculated with H_2O or NJ01 (OD_{600} = 0.5) and spray inoculated with *Pst* (OD_{600} = 0.2). Disease symptoms were photographed at 5 dpi, and bacterial titers were measured at 3 dpi.

(H and I) Stomatal aperture in leaves of Col-0 and *nced3 nced5* plants root inoculated with NJ01 (OD_{600} = 0.5) and/or spray inoculated with *Pst* (OD_{600} = 0.1). Stomatal images were taken at 3 hpi. The results are shown as mean ± SEM (n = 60 stomata). Different letters indicate significant differences at $p < 0.05$, as determined by one-way ANOVA with Tukey's multiple-comparisons test. Uppercase letters indicate comparisons between genotypes. The experiment was performed three times with similar results. Scale bars, 5 μm.

16. Melotto, M., Underwood, W., Koczan, J., Nomura, K., and He, S.Y. (2006). Plant stomata function in innate immunity against bacterial invasion. Cell *126*, 969–980.

17. Zeng, W., and He, S.Y. (2010). A prominent role of the flagellin receptor FLAGELLIN-SENSING2 in mediating stomatal response to *Pseudomonas syringae* pv *tomato* DC3000 in Arabidopsis. Plant Physiol. *153*, 1188–1198.

18. Berens, M.L., Wolinska, K.W., Spaepen, S., Ziegler, J., Nobori, T., Nair, A., Krüler, V., Winkelmüller, T.M., Wang, Y., Mine, A., et al. (2019). Balancing trade-offs between biotic and abiotic stress responses through leaf age-dependent variation in stress hormone cross-talk. Proc. Natl. Acad. Sci. USA *116*, 2364–2373.

19. Cao, F.Y., Yoshioka, K., and Desveaux, D. (2011). The role of ABA in plant-pathogen interactions. J. Plant Res. *124*, 489–499.

20. Eulgem, T., Rushton, P.J., Robatzek, S., and Somssich, I.E. (2000). The WRKY superfamily of plant transcription factors. Trends Plant Sci. *5*, 199–206.

21. Jiang, C.H., Huang, Z.Y., Xie, P., Gu, C., Li, K., Wang, D.C., Yu, Y.Y., Fan, Z.H., Wang, C.J., Wang, Y.P., et al. (2016). Transcription factors WRKY70 and WRKY11 served as regulators in rhizobacterium *Bacillus cereus* AR156-induced systemic resistance to *Pseudomonas syringae* pv. *tomato* DC3000 in Arabidopsis. J. Exp. Bot. *67*, 157–174.

22. Xu, X., Chen, C., Fan, B., and Chen, Z. (2006). Physical and functional interactions between pathogen-induced Arabidopsis WRKY18, WRKY40, and WRKY60 transcription factors. Plant Cell *18*, 1310–1326.

23. Chen, H., Lai, Z., Shi, J., Xiao, Y., Chen, Z., and Xu, X. (2010). Role of Arabidopsis WRKY18, WRKY40 and WRKY60 transcription factors in plant responses to abscisic acid and abiotic stress. BMC Plant Biol. *10*, 281.

24. Wagner, S., Stuttmann, J., Rietz, S., Guerois, R., Brunstein, E., Bautor, J., Niefind, K., and Parker, J.E. (2013). Structural basisi for signaling by exclusive EDS1 heteromeric complexes with SAG101 or PAD4 in plant innate immunity. Cell Host Microbe *14*, 619–630.

25. Wang, D., Wei, L., Liu, T., Ma, J., Huang, K., Guo, H., Huang, Y., Zhang, L., Zhao, J., Tsuda, K., and Wang, Y. (2023). Suppression of ETI by PTI priming to balance plant growth and defense through a MPK3/MPK6-WRKYs-PP2Cs module. Mol. Plant *16*, 903–918.

26. Bhandari, D.D., Lapin, D., Kracher, B., von Born, P., Bautor, J., Niefind, K., and Parker, J.E. (2019). An EDS1 heterodimer signalling surface enforces timely reprogramming of immunity genes in Arabidopsis. Nat. Commun. *10*, 772.

27. Birkenbihl, R.P., Kracher, B., Roccaro, M., and Somssich, I.E. (2017). Induced genome-wide binding of three Arabidopsis WRKY transcription factors during early MAMP-triggered immunity. Plant Cell *29*, 20–38.

28. Cui, H., Qiu, J., Zhou, Y., Bhandari, D.D., Zhao, C., Bautor, J., and Parker, J.E. (2018). Antagonism of Transcription Factor MYC2 by EDS1/PAD4 Complexes Bolsters Salicylic Acid Defense in Arabidopsis Effector-Triggered Immunity. Mol. Plant *11*, 1053–1066.

29. Aarts, N., Metz, M., Holub, E., Staskawicz, B.J., Daniels, M.J., and Parker, J.E. (1998). Different requirements for EDS1 and NDR1 by disease resistance genes define at least two R gene-mediated signaling pathways in Arabidopsis. Proc. Natl. Acad. Sci. USA *95*, 10306–10311.

30. Jing, B., Xu, S., Xu, M., Li, Y., Li, S., Ding, J., and Zhang, Y. (2011). Brush and spary: a high-throughput systemic acuqired resistance assay suitable for large-scale genetic screening. Plant Physiol. *157*, 973–980.

31. Rietz, S., Stamm, A., Malonek, S., Wagner, S., Becker, D., MedinaEscobar, N., Corina Vlot, A., Feys, B.J., Niefind, K., and Parker, J.E. (2011). Different roles of Enhanced Disease Susceptibility1 (EDS1) bound to and dissociated from Phytoalexin Deficient4 (PAD4) in Arabidopsis immunity. New Phytol. *191*, 107–119.

32. Falk, A., Feys, B.J., Frost, L.N., Jones, J.D., Daniels, M.J., and Parker, J.E. (1999). EDS1, an essential component of R gene-mediated disease resistance in Arabidopsis has homology to eukaryotic lipases. Proc. Natl. Acad. Sci. USA *96*, 3292–3297.

33. Pandey, S.P., and Somssich, I.E. (2009). The role of WRKY transcription factors in plant immunity. Plant Physiol. *150*, 1648–1655.

34. Wang, H., Song, S., Gao, S., Yu, Q., Zhang, H., Cui, X., Fan, J., Xin, X., Liu, Y., Staskawicz, B., and Qi, T. (2024). The NLR immune receptor ADR1 and lipase-like proteins EDS1 and PAD4 mediate stomatal immunity in Nocotiana benthamiana and Arabidopsis. Plant Cell *36*, 427–446.

35. Wang, D., Amornsiripanitch, N., and Dong, X. (2006). A genomic approach to identify regulatory nodes in the transcriptional network of systmic acquired resistance in plants. PLoS Pathog. *2*, e123.

36. Shang, Y., Yan, L., Liu, Z.Q., Cao, Z., Mei, C., Xin, Q., Wu, F.Q., Wang, X.F., Du, S.Y., Jiang, T., et al. (2010). The Mg-Chelatease H subunit of Arabidopsis antagonizes a group of WRKY transcription repressors to relieve ABA-responsive genes of inhibition. Plant Cell *22*, 1909–1935.

37. Liu, S., Kracher, B., Ziegler, J., Birkenbihl, R.P., and Somssich, I.E. (2015). Negative regulation of ABA signaling by WRKY33 is critical for Arabidopsis immunity towards *Botrytis cinerea* 2100. Elife *4*, e07295.

38. Knoester, M., Pieterse, C.M., Bol, J.F., and Van Loon, L.C. (1999). Systemic resistance in Arabidopsis induced by rhizobacteria requires ethylene-dependent signaling at the site of application. Mol. Plant Microbe Interact. *12*, 720–727.

39. Kazan, K., and Manners, J.M. (2013). MYC2: The Master in Action. Mol. Plant *6*, 686–703.

40. Sáenz-Mata, J., Salazar-Badillo, F.B., and Jiménez-Bremont, J.F. (2014). Transcriptional regulation of Arabidopsis thaliana WRKY genes under interaction with beneficial fungus Trichoderma atroviride. Acta Physiol. Plant. *36*, 1085–1093.

41. Lapin, D., Kovacova, V., Sun, X., Dongus, J.A., Bhandari, D., von Born, P., Bautor, J., Guarneri, N., Rzemieniewski, J., Stuttmann, J., et al. (2019). A coevolved EDS1-SAG101-NRG1 module mediates cell death signaling by TIR-domain immune receptors. Plant Cell *31*, 2430–2455.

42. Wildermuth, M.C., Dewdney, J., Wu, G., and Ausubel, F.M. (2001). Isochorismate synthase is required to synthesize salicylic acid for plant defence. Nature *414*, 562–565.

43. Wang, Y., Schuck, S., Wu, J., Yang, P., Döring, A.C., Zeier, J., and Tsuda, K. (2018). MAPK3/6-WRKY33-Pipecolic acid regulation loop contributes to systemic acquired resistance. Plant Cell *30*, 2480–2494.

44. Wu, J., Mei, X., Zhang, J., Ye, L., Hu, Y., Chen, T., Wang, Y., Liu, M., Zhang, Y., and Xin, X.F. (2023). CURLY LEAF modulates apoplast liquid water status in Arabidopsis leaves. Plant Physiol. *193*, 792–808.

45. Grabherr, M.G., Haas, B.J., Yassour, M., Levin, J.Z., Thompson, D.A., Amit, I., Adiconis, X., Fan, L., Raychowdhury, R., Zeng, Q., et al. (2011). Full-length transcriptome assembly from RNA-Seq data without a reference genome. Nat. Biotechnol. *29*, 644–652.

46. Yamaguchi, N., Winter, C.M., Wu, M.F., Kwon, C.S., William, D.A., and Wagner, D. (2014). PROTOCOLS: Chromatin immunoprecipitation from Arabidopsis tissues. Arabidopsis Book *12*, e0170.

47. Huang, L., and Zhang, C. (2021). Microscale thermophoresis (MST) to detect the interaction between purified protein and small molecule. Methods Mol. Biol. *2213*, 187–193.

48. Yu, L., He, W., Xie, J., Guo, R., Ni, J., Zhang, X., Xu, Q., Wang, C., Yue, Q., Li, F., et al. (2019). In vitro biochemical assays using biotin labels to study protein-nucleic acid interactions. JoVE, e59830.

STAR★METHODS

KEY RESOURCES TABLE

REAGENT or RESOURCE	SOURCE	IDENTIFIER
Antibodies		
EDS1 Rabbit Antibody	AgriSera	Cat# AS13 2751; RRID: AB_3076639
PAD4 Rabbit Antibody	Phytoab	Cat# PHY1539S; RRID: AB_3083005
SAG101 Rabbit Antibody	Phytoab	Cat# PHY1539S; RRID: AB_3083006
HA Mouse Antibody	Sigma-Aldrich	Cat# H9658; RRID: AB_260092
GST Mouse Antibody	Sangon Biotech	Cat# D190101; RRID: AB_2940945
His Rabbit Antibody	Sangon Biotech	Cat# D191001; RRID: AB_2940946
Goat anti Rabbit IgG	Sangon Biotech	Cat# D110058; RRID: AB_2940954
Goat anti Mouse IgG	Sangon Biotech	Cat# D110087; RRID:AB_2940948
Bacterial and virus strains		
Escherichia coli strain DH5a	Wang lab stock	N/A
Agrobacterium tumefaciens strain GV3101	Wang lab stock	N/A
Pseudomonas syringae pv. *tomato DC3000*	Wang lab stock	N/A
Xanthomonas oryzae pv. oryzicola (*Xoc*)	Wang lab stock	N/A
Xanthomonas oryzae pv. oryzae (*Xoo*)	Wang lab stock	N/A
Bacillus cereus strain NJ01	Wang lab stock	N/A
Chemicals, peptides, and recombinant proteins		
TRIzol	Thermo Fisher Scientific	Cat# 15596026
Bovine Serum Albumin (BSA)	Sigma-Aldrich	Cat# A8806
Protease Inhibitor Cocktail	Sigma-Aldrich	Cat# S8830
DTT	Sigma-Aldrich	Cat# 3483-12-3
PMSF	Sigma-Aldrich	Cat# 329-98-6
Critical commercial assays		
EMSA assay kit	Thermo Fisher Scientific	Cat# 20148
RevertAid RT Reverse Transcription Kit	Thermo Fisher Scientific	Cat# K1691
AceQ Universal SYBR qPCR Master Mix	Vazyme	Cat# Q511-02
Deposited data		
RNA sequencing data	This paper	PRJCA023793
RNA sequencing data	Bhandari et al.[26]	GSE116269
CHIP sequencing data	Birkenbihl et al.[27]	GSE85922
Experimental models: Organisms/strains		
Arabidopsis thaliana: Col-0	Arabidopsis Biological Resource Center	N/A
Arabidopsis thaliana: *eds1*	Lapin et al.[41]	N/A
Arabidopsis thaliana: *pad4*	Lapin et al.[41]	N/A
Arabidopsis thaliana: *sag101*	Lapin et al.[41]	N/A
Arabidopsis thaliana: *pad4 sag101*	Lapin et al.[41]	N/A
Arabidopsis thaliana: *eds1 pad4 sag101*	Lapin et al.[41]	N/A
Arabidopsis thaliana:P_{EDS1}::*gEDS1-YFP eds1*	Wagner et al.[24]	N/A
Arabidopsis thaliana: P_{EDS1}::*gEDS1*^{LLIF}-*YFP eds1*	Wagner et al.[24]	N/A
Arabidopsis thaliana: *wrky18*	Xu et al.[22]	N/A
Arabidopsis thaliana: *wrky18/40/60*	Xu et al.[22]	N/A
Arabidopsis thaliana: P_{WRKY18}::*WRKY18-HA wrky18*	Birkenbihl et al.[27]	N/A
Arabidopsis thaliana: P_{35S}:*YFP-HA*	Wang et al.[25]	N/A
Arabidopsis thaliana: *ics1/sid2*	Wildermuth et al.[42]	N/A

(*Continued on next page*)

Continued		
REAGENT or RESOURCE	SOURCE	IDENTIFIER
Arabidopsis thaliana: *nced3/5*	Liu et al.[37]	N/A
Oryza sativa L. Zhonghua11	China Rice Data Center	N/A
Oryza sativa L. *eds1*	This paper	N/A
Oligonucleotides		
All primers are listed in Table S5	This paper	N/A
Software and algorithms		
GraphPad Prism version 9.0	GraphPad Software	https://www.graphpad.com/
ImageJ	National Institutes of Health	https://imagej.nih.gov/ij/
SPSS version 25.0	IBM	https://www.ibm.com/analytics/spss-statistics-software
Nikon NIS-Elements Viewer	Nikon	https://www.microscope.healthcare.nikon.com/products/software/nis-elements/viewer

RESOURCE AVAILABILITY

Lead contact

Further information and requests for resources and reagents should be directed to and will be fulfilled by the lead contact, Yiming Wang (ymwang@njau.edu.cn).

Materials availability

All unique/stable reagents generated in this study are available from the lead contact with a completed materials transfer agreement.

Data and code availability

The transcriptome result has been uploaded to the National Center for Biotechnology Information (NCBI) and are publicly available as of the date of publication. Accession numbers are listed in the key resources table.

This paper does not report original code.

Any additional information required to reanalyze the data reported in this paper is available from the lead contact upon request.

EXPERIMENTAL MODEL AND SUBJECT PARTICIPANT DETAILS

Plant materials and growth conditions

Arabidopsis thaliana accession Col-0 was used as the wild type. Mutants of *eds1-2*, *pad4*, *sag101*, *pad4 sag101*, and *eds1 pad4 sag101*,[41] P_{EDS1}*::gEDS1-YFP eds1-2*,[24] P_{EDS1}*::EDS1*^{LLIF}*-YFP eds1-2*,[24] *wrky18*, *wrky18/40/60*,[22] *ics1/sid2*,[42] *nced3 nced5*,[37] and P_{WRKY18}*::WRKY18-HA wrky18*[27] were described previously. Arabidopsis was grown in a growth chamber at 22°C under a 8-h-light period with 65% relative humidity. Four-week-old plants were used for bacterial infection and stomatal measurements.

Rice plants were grown in a growth chamber at 28°C under a 16-h-light period with 65% relative humidity. *Oseds1* mutant was generated in *Oryza sativa* pv. *oryzae* cv. Zhonghua 11 (ZH11) background (Figure S7).

METHOD DETAILS

Bacterial strains, infection and bacterial growth analysis

B. subtilis strain NJ01 was cultured at 28°C for 24 h on Luria-Bertani (LB) plate. A single colony from a freshly streaked plate was picked and inoculated into LB broth and incubated at 28°C for 16 h. Bacterial cells were subsequently collected by centrifugation, washed twice with sterile water, and re-suspended in sterile water to a final density of ~0.5 OD_{600}. Root inoculation of NJ01 was done by pipetting 10 mL of ~0.5 OD_{600} aqueous bacterial suspension to Arabidopsis and rice. *Pseudomonas syringae* pv. *tomato* DC3000 (*Pst*) was cultivated as described previously (Tsuda et al., 2013). Bacterial cells were washed with water, diluted to the appropriate density in 10 mM $MgCl_2$, and sprayed (OD_{600} = 0.2) or infiltrated (OD_{600} = 0.001) into Arabidopsis leaves. Bacterial titer was measured as described previously (Wang et al., 2018). *Xanthomonas oryzae* pv. *oryzae* (*Xoo*) inoculation was applied leaf clipping method. Briefly, dip scissor tips into the *Xoo* suspension (OD_{600} = 0.5) and cut the leaf tip (approximately 2–3 cm) away from the leaf. Infection phenotype was detected at 14 days post inoculation (dpi). *Xanthomonas oryzae* pv. *oryzicola* (*Xoc*) suspensions (OD_{600} = 0.5) were sprayed on the leaves of two-week-old rice seedlings. Infection phenotype was detected at 5 days post inoculation (dpi).

RNA extraction and qPCR analysis

Total RNA from Arabidopsis and rice leaves were extracted and qRT-PCR analysis were performed as described previously.[43] In brief, RNA was extracted by TRIzol solution (Therom Fisher Scientific), and then treated with DNase, and 1 mg of total RNA was reverse transcribed using SuperScript II first-strand synthesis system (Therom Fisher Scientific) with an oligo(dT_{20}) primer. Real-time DNA amplification was monitored using Bio-Rad iQ5 optical system software (Bio-Rad). Primers used for qRT-PCR was listed in Table S5.

Stomatal apartural analysis

Leaves of four-week-old Arabidopsis plants were used for the stomatal measurement. The abaxial epidermis was obtained by epidermal peeling. To maintain the accuracy of the experiments, the images of the stoma at indicated times were taken quickly using a Nikon camera (Nikon C2+) with DAPI and light channels as described before.[44] The stomatal aperture was measured using ImageJ.

Transcriptome and data analysis

Soil-grown 4-week-old plants were root-inoculated either with 10 mL of ~0.5 OD_{600} aqueous bacterial suspension for 3 h or with sterile water as negative control. Individual leaves from plants were harvested and total RNA was extracted by TRIzol solution (Thermo Fisher Scientific) followed by DNase treatment. The RNA sequencing library of the two treatments was constructed and the transcriptome sequencing was processed by Beijing Genomics Institute (BGI), China, using the HiSeqTM 2500 platform. The results have been uploaded to the National Genomics Data Center BioProject database (https://ngdc.cncb.ac.cn/) in FASTQ format (BioProject accessions: PRJCA023793; BioSample accessions: SAMC3400684, SAMC3400685, SAMC3400686, SAMC3400687, SAMC3400688, SAMC3400689). The clean reads were acquired by Illumina Pipeline Software, and the adaptors and low-quality reads (Q < 20) were removed using Perl scripts. *De novo* assembly of the transcripts was performed by the Trinity method.[45] For assembled genes, the longest contigs were filtered, clustered into the non-redundant transcripts, and were defined as unigenes. Unigenes were then produced by mapping the data back to the contigs of the clean reads. Unigenes with significant expression were searched against the non-redundant protein sequence database using the NCBI BlastX (E-value $\leq 10^{-5}$). The blast result was mapped to UniProt, from which GO terms were extracted. Unigenes were further searched against several databases, such as the Swiss-Prot, the KEGG pathway database, and the GO database to acquire their putative functions (Table S2).

RNA-seq and ChIP-seq re-analysis processing

The RNA-seq data of Col-0 and *eds1* were retrieved from Bhandari et al.,[26] while ChIP-seq data of WRKY18 and WRKY40 were downloaded from Birkenbihl et al.[27] Low-quality reads from RNA-seq and ChIP-seq were removed with TrimGalore (version 0.6.6). The clean reads were mapped to TAIR10 using Hisat2 (version 2.2.1) and Bowite2 (version 2.3.5.1), respectively and the uniquely mapped reads were used for subsequent analysis. For RNA-seq, differentially expressed genes were evaluated using the DESeq2 package in R with an adjusted p value <0.05. For ChIP-seq, PCR duplicates were filtered using SAMTools (version 1.14), and the unique reads of high quality were used to call peak with MACS2.

Protein extraction and immunoblot analysis

Four-week-old plants were used for protein extraction. Total protein was extracted from leaf tissue after grinding in liquid nitrogen with protein extraction buffer (50 mM Tris-Cl pH 7.6, 5 mM EDTA, 5 mM EGTA, 2 mM DTT with protein phosphatase inhibitor and protease inhibitor cocktail). Protein accumulation of EDS1 was detected by anti-EDS1 antibody (Agrisera, 1:10000). Signals were detected using a SuperSignal West Femto Trial Kit (Thermo FIsher Scienctific). Ponceau S staining of the membrane served as a loading control.

Bimolecular fluorescence complementation (BiFC) assay

For BiFC assay, the coding sequences of *EDS1*, *PAD4*, *SAG101* and *WRKY18* were cloned into *pUb-nYFP* and *pUb-cYFP* vector, respectively. The constructions were transformed into *Agrobacterium tumefaciens* strain GV3101. The transformed *A. tumefaciens* were infiltrated into *Nicotiana benthamiana* leaves at OD_{600} = 0.8. Images were taken under a confocal laser-scanning microscope (Nikon C2+) at 48 hpi.

Co-immunoprecipitation (Co-IP)

Co-IP assay was performed in 35S:GFP-HA and 35S:WRKY18-HA plants. Two g leaf samples were ground in liquid nitrogen and total proteins were extracted following the methods described above and then incubated with Pierce Anti-HA Magnetic Beads (Thermo FIsher Scienctific) overnight. The beads were collected by Magnetic frame (Thermo FIsher Scienctific) and then washed five times with cold 1xPBS (containing 0.01% Tween 20). Proteins were released from the beads by incubating at 100°C for 10 min with 60 μL 1xPBS. Immune precipitates were separated by SDS–PAGE gels and detected by immunoblotting with with anti-EDS1 (Agrisera, 1:2000), anti-PAD4 (PhytoAB, 1:1000), anti-SAG101 (PhytoAB, 1:1000) and anti-HA (Sigma, 1:5000) antibodies, respectively.

Chromatin immunoprecipitation (ChIP) assay

ChIP assay was performed as described before.[46] Briefly, Four-week-old plant was root-inoculated with NJ01, and leaf samples were collected at 3 h post inoculation. Five g of seedling tissue was harvested and cross-linked with 1% (v/v) formaldehyde solution in 1× PBS under a vacuum for 12 min. Remove formaldehyde and add 10 mL 0.125 M glycine solution (quenches the cross-linker) under a vacuum for 3 min and ground in liquid nitrogen. Subsequently, the chromatin isolation were sonicated, and immunoprecipitated with monoclonal anti-HA antibodies (Sigma). The ChIP DNA and input DNA were purified using a PCR purification kit (Qiagen) for qRT-PCR analysis. Primers used for qPCR were listed in Table S5.

Yeast-two-hybride assay

The coding sequences of full length *WRKY18* was cloned into the pGBKT7 vector (Clontech) to fuse with the GAL4 DNA binding domain (BD). The *EDS1*, *PAD4* and *SAG101* coding sequences were cloned into pGADT7 vector individually to fuse with the GAL4 activation domain (AD). The yeast strain Y2H gold (Clontech) was transformed with different combinations of the bait and prey constructs. The yeast transformants were selected on the synthetic defined (SD) yeast leucin and tryptophan dropout medium (SD/-L-T) for 3 days at 30°C. Weak and strong interactions were determined through plating the yeast transformants selected from SD/-L-T medium onto the leucine, tryptophan and histidine dropout medium (SD/-L-T-H), and allowed by 3–4 days growth at 30°C.

Microscale thermophoresis (MST) analysis

MST assays were performed using Monolith NT.115 (NanoTemper Technologies, Germany) as described previously.[47] Briefly, target DNA was fluorescently labeled with Cy3 (NanoTemper Technologies) via amine conjugation. For detecting the binding affinity, 10 μM of fluorescently labeled protein in label buffer (130 mM $NaHCO_3$, 50 mM NaCl) was titrated against increasing concentrations of unlabeled ligand. The samples were loaded into MST premium-coated capillaries (Monolith NT.115 MO-K005, Germany) and measured at 25°C with 80% MST power and 20% LED power. Data were analyzed using Nano Temper Analysis Software (NanoTemper Technologies, Germany).

Electrophoresis mobility shift assay (EMSA)

EMSA was performed as described before.[48] Briefly, 1μg WRKY18-His protein and 1μg EDS1-GST or GST protein were incubated with 1 μmol biotin-labeled probe DNA and 1 μg Poly (dI•dC) (Thermo Fisher) in binding buffer (50 mM Tris HCl at pH 7.5, 2 mM $MgCl_2$, 50 mM NaCl, 10 mM EDTA, 1 mM dithiothreitol, 10% glycerol, and 0.01% NP-40). After 20 min incubation at room temperature, the mixtures were loaded onto a 6% native acrylamide gel in 0.5×TBE buffer and electrophoresed at 4°C. After electrophoresis, crosslink the samples by irradiating the membrane 120 mJ/cm^2 using a commercial UV-light crosslinking instrument equipped with 254 nm bulbs. And then detect Biotin-labeled DNA by Chemiluminescence.

Determination of phytohormone levels

Quantifications of SA and ABA levels in the leaves of four-week-old plants were carried out through liquid chromatography–tandem mass spectrometry by the Guo Cang Jian service center (Targetcrop). In brief, the fresh plant materials were freeze-dried in liquid nitrogen and stored at −80°C until use. The dried plant materials were powdered in a mill. For the quantification of SA and ABA levels, 100 mg of dried leaf powders was homogenized in 1.5 mL mixed methanol:H_2O (80:20, v/v) solution. The resulting extract was vortexed and ultrasound for 30 min, and then placed under 4°C for 12 h. Supernatants were collected from different samples after centrifugation, and the residues were re-extracted in 1 mL methanol through ultrasound for 30 min followed by precipitation via centrifugation. The resulting supernatants were mixed, dried through evaporation under nitrogen gas stream, and reconstituted in methanol. The solution was then filtered through a 0.22-μm filter. The samples were analyzed using a Triple Quadrupole 4500 LC/MS/MS System (AB Sciex) equipped with an ESI ion source and a Hypersil Gold C18 column (3 μm, 2.1 mm × 100 mm).

Accession numbers

EDS1, AT3G48090; *PAD4*, AT3G52430; *SAG101*, AT5G14930; *WRKY18*, AT4G31800; *WRKY40*, AT1G80840; *WRKY60*, AT2G25000; *ICS1*, AT1G74710; *NCED3*, AT3G14440; *NCED5*, AT1G30100; *OsEDS1*, LOC_Os09g22450.

QUANTIFICATION AND STATISTICAL ANALYSIS

Statistical analyses were performed with Graphpad Prism 9.0 software (https://www.graphpad.com/). For stomatal apartural analysis, the results are shown as means ± SEMs (n = 60 stomata). Different letters indicate significant differences at $p < 0.01$, as determined by one-way ANOVA with Tukey's multiple comparisons test. For other data, the results are presented as mean ± SD, and 'n' represents number of samples from at least 3 replicates. One-way ANOVA with Tukey's test was used for multiple comparisons. Two tailed Student's t test was used to compare means for two groups. Differences were considered statistically significant when $p < 0.05$. Details about the statistical analyses are described in the figure legends.